공학석사 학위논문

Synthesis of choline-based levelers with different number of quaternary ammoniums and their application on Cu electrodeposition

다른 개수의 4 가 암모늄 치환체를 가지는 콜린 기반 평탄제의 합성과 구리 전해도금에서의 적용

2022 년 8 월

서울대학교 대학원

화학생물공학부

김 정 아

Synthesis of choline-based levelers with different number of quaternary ammoniums and their application on Cu electrodeposition

By

Jungah Kim

August 2022

Thesis Advisor: Young Gyu Kim

Synthesis of choline-based levelers with different number of quaternary ammoniums and their application on Cu electrodeposition

지도 교수 김 영 규

이 논문을 공학석사 학위논문으로 제출함
2022 년 8 월

서울대학교 대학원
화학생물공학부
김 정 아

김정아의 공학석사 학위논문을 인준함
2022 년 6 월

위 원 장 백 승렬 (인)

부위원장 김 영규 (인)

위 원 유 동원 (인)

Abstract

Synthesis of choline-based levelers with different number of quaternary ammoniums and their application on Cu electrodeposition

Jung Ah Kim
School of Chemical and Biochemical Engineering
The Graduate School
Seoul National University

As 3D packaging technology for high-functionality electric devices has been developing, effective electric interconnecting methods are also expected. Through-silicon via (TSV) is the representative 3D integration technology connecting stacked dies through vias filled with conductive material to work as the interconnection of electric signal path. Therefore, defect-free via filling should be achieved for reliability of electronics, and copper electrodeposition has been used as filling process.

The use of organic additives is indispensable for Cu electrodeposition. Leveler is one of the organic additives which regulates rate of electrodeposition by its selective adsorption

behavior on Cu surface. According to previous research, the convection dependent adsorption behavior of leveler is affected by its molecular structure, especially by the quaternary ammonium functional groups. In this thesis, structure–property relationship leveler for Cu electrodeposition was studied to develop levelers for optimized additive combination.

Three levelers having different number of quaternary ammonium groups (Lev-A1, Lev-A2, and Lev-A3) were synthesized, and their electrochemical properties on Cu electrodeposition were analyzed. Convection-dependent adsorption behavior of levelers was observed, and the property was enhanced by number of quaternary ammonium groups. In via filling test, Lev-A3 resulted in most effective filling with highest thickness ratio value and superconformal filling profile. In conclusion, three levelers having one, two, and three quaternary ammonium groups were successfully synthesized, and the influence of quaternary ammonium group on convection dependent adsorption was studied.

Keyword: 3D packaging, Cu electrodeposition, Leveler, Convection-dependent adsorption behavior, Structure-property relationship, Quaternary ammonium functional group

Student Number: 2020-26086

Table of Contents

LIST OF FIGURES

LIST OF TABLES

LIST OF SCHEMES

LIST OF ABBREVIATIONS

ALD	Atomic layer deposition
CEAC	Curvature enhanced accelerator coverage
Cu	Copper
CVD	Chemical vapor deposition
DMF	Dimethylformamide
Et_2O	Diethyl ether
EtOAc	Ethyl acetate
IC	Integrated circuit
LSV	Linear sweep voltammetry
*m*CPBA	*meta*-chloroperoxybenzoic acid
MeOH	Methanol
NMR	Nuclear magnetic resonance
PCB	Printed circuit board
PEG	Polyethylene glycol
PPG	Polypropylene glycol
PVD	Physical vapor deposition
RDE	Rotation disk electrode
SPS	bis-(3-sulfopropyl)-disulfide disodium salt
TEG	Triethylene glycol
THF	Tetrahydrofuran
TMS	Tetramethylsilane
TSV	Through-silicon via

1. Introduction

1.1 3D interconnection technology

As the demand of high-performance electronics for artificial intelligence (AI), neural processing unit (NPU), super computer, and self-driving car has been increasing significantly, the importance of 3D interconnection technology is also increasing rapidly. These high-functionality electric devices should perform multiple functions simultaneously even with the smaller sizes. 3D integration technology enables devices to achieve complex and multiple functions simultaneously by the vertical stacking of modules.[1] In addition, 3D packaging is the vertical interconnection of devices which allows them to function as one integrated device but still be able to perform various functions.[2,3] Consequently, the 3D integration has proven its advantages over 2D interconnection, such as increased functionality and improved performance with reduced form factor.[3] 3D stacking technologies have developed from the interconnection by wire bonding to the interconnection through the board. The conventional method is wire bonding which connects carrier PCB board and dies with bonding wires or flip chip bonding which use bumps for internal connection (Fig. 1a)[3]. The bonding methods have developed to accomplish high area efficiency by reducing interconnection length and width of bonding, which result in shorter signal transfer time and lower power consumption. For example, through-silicon via (TSV) is the 3D integration technology

connecting adjacent dies with small electrical connections called vias, the vertical interconnections through dies (Fig. 1b)[2,3]. In TSV technology, vias are formed then filled with electrically conductive materials to work as the path of electric signal.[4,5] For this reason, it is essential to achieve defect-free TSV filling to ensure the reliability of electric devices.[6] 3D integrated circuit (IC) package with TSV consists of assembled IC substrates connected through multiple via hole connections. For instance, high bandwidth memory (HBM) consists of multiple DRAM dies stacked through several thousands of TSV and micro-bumps, and it allows faster speed, high bandwidth, and improved I/O power efficiency.[7,8] Likewise, high density interconnect (HDI) board is a type of PCB with higher wiring density than conventional PCB, and it consists of smaller via called microvia.[9] In terms of via filling, copper is most widely used filling material because of its low electric resistance and compatibility to conventional multilayer interconnects related to aluminum or tungsten.[6,10,11,12] Copper filling is performed through electrodeposition process, and the effective copper filling is proceeded from the bottom of vias then through the top, which called bottom-up filling (Fig. 2)[10,12,13]. Bottom-up filling, also called as superconformal filling, is a preferable filling method to avoid incomplete filling such as via seams or voids.[10] Consequently, the reliability of Cu electrodeposition depends on optimized electrical performance which related with filling efficiency; filling material and method. On the other hand, as the size of circuits become miniaturized, the novel Cu-based interconnecting process has to be implemented to enable copper etching correspondingly.

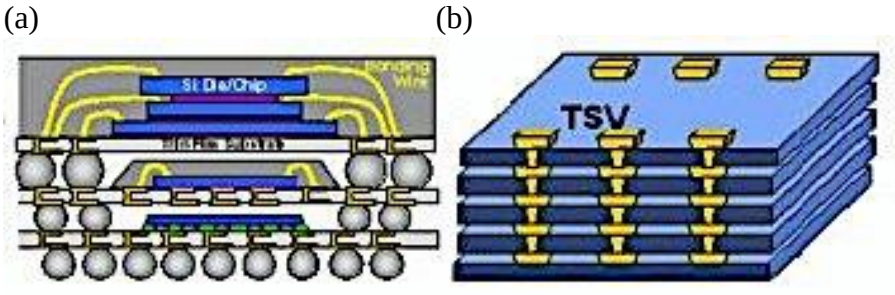

Figure 1. 3D packaging technology. (a) Packaging based on wiring bonding and flip-chip bonding and (b) Die-to-die bonding by TSV

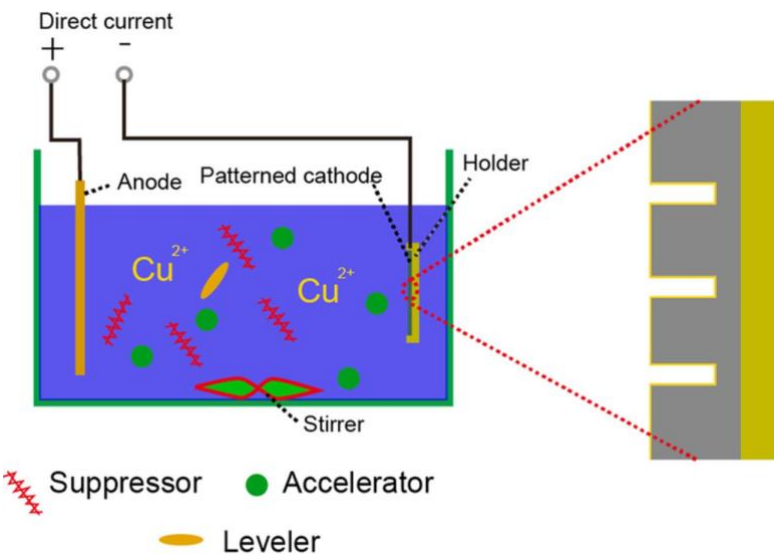

Figure 2. Copper electrodeposition environment for via filling experiment

1.2 Cu electrodeposition

To establish defect-free metallization in interconnection, proper filling materials and plating methods should be selected carefully. In addition, decent filling metal has to be chosen since resistance-capacitance (RC) delay could be caused in miniaturized electronics.[14] At one time, aluminum was recognized as proper interconnecting metal because of low electric resistivity and great etchability. However, since the early 1990s, copper replaced aluminum owing to its even lower electric resistivity and higher resistivity to electromigration (EM) (Table. 1)[14,15]. Thus, copper filling is able to produce better filling with reduced probability of voids or hillock formation even in smaller line dimension. On the other hand, as the size of circuits become miniaturized, the novel Cu-based interconnecting process has to be implemented to enable copper etching correspondingly.[16,17] For instance, the Cu-damascene process was developed to prevent copper diffusion to the silicon oxide inner layer. In Cu-damascene, diffusion barrier and seed layers have to be developed on the interlayer dielectric (ILD) before copper filling (Fig. 3)[16]. After copper gap-filling by copper electrodeposition, the process is completed with chemical metal polishing (CMP) to planarize then finalize copper metallization.[17-19] In terms of plating method, copper electrodeposition is employed, even though several candidates such as physical vapor deposition (PVD), chemical vapor deposition (CVD), atomic layer deposition (ALD), and electroless deposition exist. To achieve defect-free filling, electrodeposition should be used considering a step coverage value, fluorine effect, yield and stability of plating.[19-22] For example,

PVD is subject to poor step coverage which lead to via seam or void formation, and ALD often results in low yield. In case of CVD, fluorine gas diffuses and reacts with Ta/TaN barrier. Electroless deposition is also not commonly used because of its instability. Electrodeposition system consists of working electrode, insoluble anode, and counter electrode.[23] During copper electrodeposition process, copper ions from plating solution reduce on the cathode by using external electron source.[24] In this circumstance, superconformal fiiling is indispensable to fulfill filling with high aspect ratio.[25,26] Superconformal filling is achieved when deposition occurs actively at the bottom of via while deposition velocity is strongly controlled at the top and the side walls (Fig. 4)[26]. If the deposition rate at the bottom related to the top of vias is not regulated adequately, subconformal filling would cause void or hillock (Fig. 4a)[23,26]. Furthermore, when the deposition would proceed at the same velocity from every position, conformal filling induces center seam would be observed (Fig. 4b)[26]. Since these defects could damage the reliability of interconnection, it is important to establish optimized electrolyte and additive combination in electrodeposition system.

Table. 1. Melting point and resistivity of metal candidates for electrodeposition

Metal	Melting point (°C)	Resistivity (ρ) at 298K (μΩ-cm)
Silver (Ag)	961	1.587
Copper (Cu)	1084	1.678
Gold (Au)	1064	2.214
Aluminum (Al)	660	2.650
Tungston (W)	3422	5.280

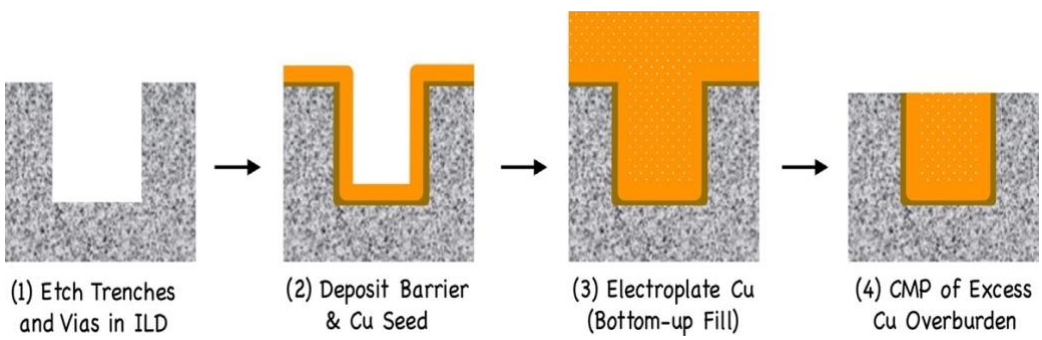

Figure 3. Schematic of the progress of interconnect fabrication by Cu electrodeposition

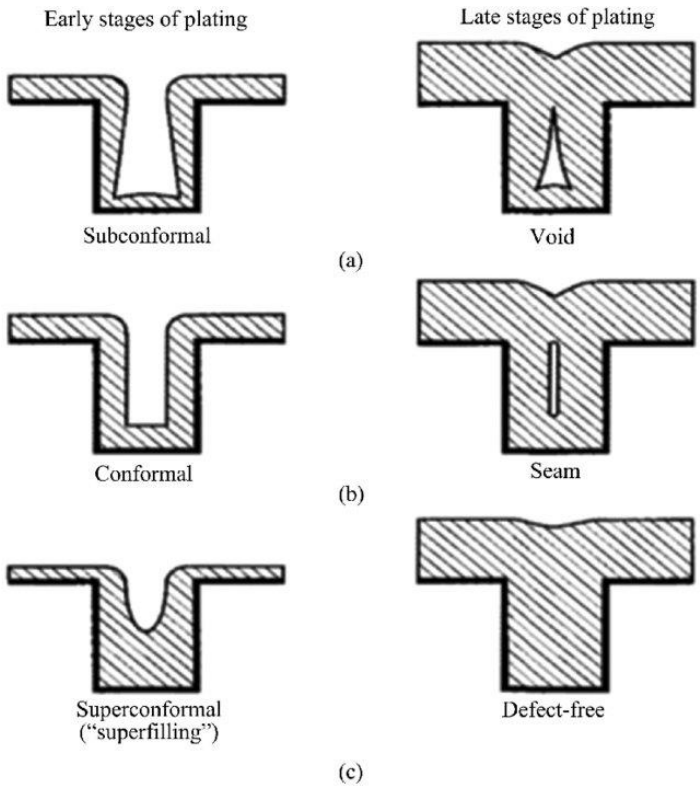

Figure 4. Schematic of possible copper filling profiles at different stages. (a) Incomplete filling with void due to faster deposition rate at the top, (b) with seam caused by uniformed deposition rate. (c) Defect-free filling achieved by faster deposition rate at the bottom

1.3 Organic additive system in Cu electrodeposition

To achieve defect-free Cu filling, organic additives are used to adjust electrodeposition rate.[27] Additive are classified as accelerator, suppressor, and leveler regarding to their electrochemical characteristics. For example, accelerator enhances Cu electrodeposition rate, and it generally contains disulfide bond or mercapto groups such as bis-(3-sulfopropyl)-disulfide disodium salt (SPS) or sodium 3-mercapto-1-propanesulfonate (MPS) (Fig. 5)[26,27]. During electrodeposition, accelerator provides electron to Cu^{2+} to form the complex (Cu-thiolate) and facilitates the reduction to Cu.[26] Conversely, suppressor plays a disrupting role by inhibiting Cu ions approaching to the deposition place.[22] Suppressors are usually polyesters containing polyethylene glycol (PEG) or propylene glycol (PPG), and their copolymers.[22] The oxygen lone-pair electrons of polyethylene group of suppressors form the complex (PEG-Cu^{+}-Cl^{-}- Cu) then adsorb on Cu surface to physically inhibit Cu reduction.[29] Therefore, the most representative suppressor is PEG with small amount of chloride ion (Cl^{-}).[22] The competitive adsorption between accelerator and suppressor on Cu surface is an effective method to explain superfilling mechanism, based on curvature enhanced accelerator coverage (CEAC) model (Fig. 6)[23,27,29,30]. According to CEAC, the stronger surfactant SPS displaces suppressor from the pre-adsorbed suppressor-Cu complex on the surface, and Cu deposition is facilitated.[31] With this enhanced deposition rate, the bottom of via becomes concave-shaped resulting in SPS accumulation.[32] Finally, the increased SPS-Cl coverage promotes deposition rate at the bottom corner, and this

mechanism called bottom-up superfilling. It has been known that decent combination of accelerator and suppressor allows successful filling with dimension below a few hundreds of nm.[22] On the other hand, leveler is a second class of suppressor used for selective inhibition along the depth of vias. For example, leveler exhibits selective inhibition effect based on convection strength which called convection-dependent adsorption. Where current is isolated due to limited mass transfer such as the inside of vias, leveler shows less inhibition effect compared to the top or side where mass transfer by diffusion or migration is substantially active.[24] The general structural features of leveler suggest that tertiary amine or quaternary ammonium functional group might be related with its convection dependent adsorption behavior. Several representative levelers including Janus Green B (JGB) and diallyl amine are shown in figure 7.[33] Addition of leveler provides three additive system (accelerator, suppressor, and leveler) which enables larger size filling such as microvia and TSV. Besides, recent studies account for the close relationship between the convection-dependent adsorption of leveler and bottom-up filling.[34] Therefore, optimized additive system should be established for defect-free bottom-up filling.

(a)

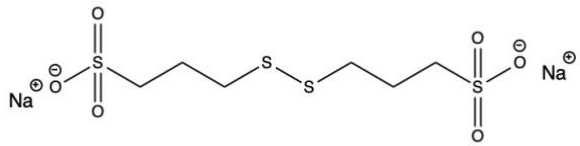

(b)

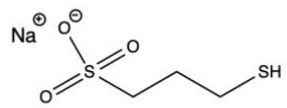

Figure 5. Molecular structures of representative accelerators for Cu electrodeposition. (a) bis-(3-sulfopropyl)-disulfide disodium salt (SPS) and (b) sodium 3-mercapto-1-propanesulfonate (MPS)

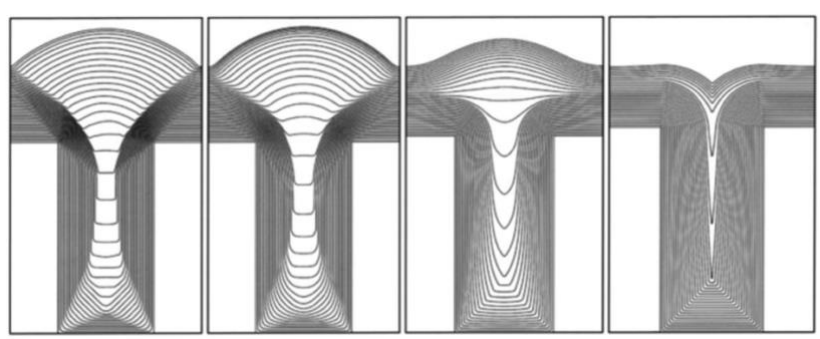

Figure 6. Gap-filling model by curvature enhanced accelerator coverage (CEAC) model

(a)

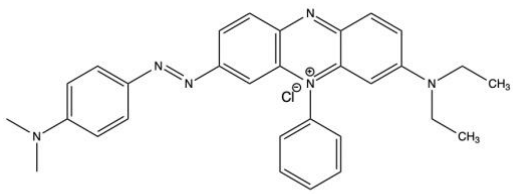

(b)

(c)

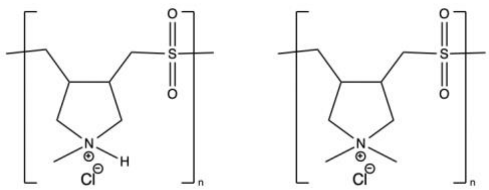

Figure 7. Molecular structures of reported levelers for Cu electrodeposition. (a) Janus Green B (JGB) and (b) N-doped aromatic heterocyclic compounds, tricyclazole (left) and 2-mercaptopyridine (right). (c) diallylamine copolymers

1.4 Structure–property relationship of leveler

From previous literatures, electrochemical features of leveler are heavily related to its structural properties.[35,36] Among others, convection–dependent adsorption behavior is the most representative property of leveler which is directly related to its adsorption ability. It is obvious that filling performance is affected by the adsorption behavior of levelers. Therefore, study of the structure–property relationship of leveler should be conducted to enhance filling performance. In our laboratory, we have synthesized triethylene glycol (TEG)–based levelers with different halide ions.[37] (TEG)–based levelers have one or more ethylene glycol units at the center and two quaternary ammoniums at both ends with halide counter ions (Fig. 8)[37]. Especially, we proposed choline–based structure since it has been showing convection–dependent adsorption behavior from electrochemical analyses.[37,] We devised the design based on three structural reasonings. First, ethylene glycol unit was adopted as the core structure since its lone pair electrons contribute to the formation of inhibition layer (PEG–Cu^{+}–Cl^{-}–Cu complex) as PEG does in suppressor.[38,39] Accordingly, ethylene glycol unit is related with inhibition strength. Next, from the choline structure, hydroxy groups are also related to the formation of PEG–Cu^{+}–Cl^{-}–Cu complex due to their oxygen lone–pair electrons.[36] Finally, quaternary ammonium groups and counter halide ions were also chosen from the choline structure.[37] As mentioned above, tertiary amine or quaternary ammonium functional groups are one of the general structural features of leveler, and they are expected to induce convection dependent adsorption since its positive charge

prevent Cu^{2+} ion from reducing on the Cu surface.[40–42] This suppressing effect would result in regular and relative copper deposition.[40] In addition, the properties of quaternary ammonium compounds are decided by their chemical structures such as functional groups and attached hydrophilic or hydrophobic groups.[40,41] Furthermore, length, counter ions, and aromaticity are all factors that affect its leveling ability.[36] Among others, I focused on the quaternary ammoniums groups to study the structure–property relationship between leveler and Cu electrodeposition. There has been research about the effect of different numbers of quaternary ammoniums in structure of leveler.[19, 43] In this thesis, three choline–based levelers having one, two and three quaternary ammoniums with bromide counter ions respectively (**Lev–A1, Lev–A2**, and **Lev–A3**) were synthesized. Then their inhibition effect on Cu electrodeposition, interaction with other additive (accelerator), and via filling performance were analyzed and compared. The objective of this study is to investigate the influence of ammonium function group on Cu electrodeposition and the structure–property relationship of leveler. Thus, this study would be further developed to give an insight for novel design of leveler.

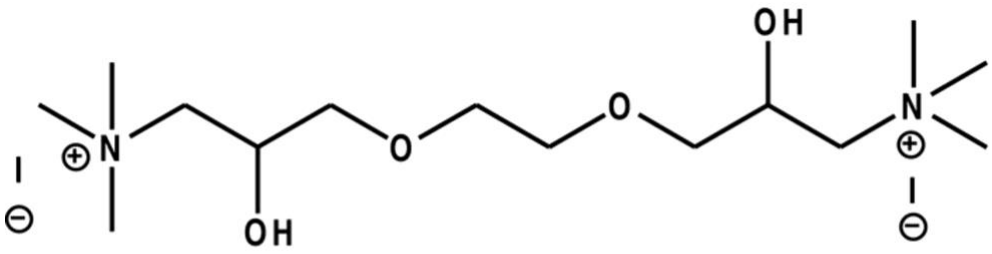

α,ω-Bis(*N,N,N*-trimethylammoniomethyl) triethylene glycol diiodide

Figure 8. Molecular structure of previously reported triethylene glycol (TEG)-based leveler

2. General Procedure for electrochemical analyses

2.1. Electrochemical analyses of synthesized levelers

All the electrochemical analyses and via filling tests were performed by Myung Hyun Lee in Professor Jae Jeong Kim's laboratory in Seoul National University. Linear sweep voltammetry (LSV) and chronopotentiometry by a potentiostat (PAR 263, EG&G Princeton Applied Research Corp.) were conducted to understand the adsorption of synthesized leveler. At 25 Celsius degree, electrolyte for Cu electrodeposition contained $CuSO_4 \cdot 5H_2O$ (0.92 M), H_2SO_4 (0.43 M), and HCl (0.82 mM). To the standard Cu plating solution (VMS), three organic additives; suppressor (PPG-PEG-PPG, M_w = 2000), accelerator (SPS) and synthesized levelers were added. The concentration of SPS was varied from 3 to 24 μM, and the concentration of PPG-PEG-PPG was fixed at 100 μM. The concentration of synthesized levelers (**Lev-A1, Lev-A2, and Lev-A3**) were 7 μM, then adjusted by the number of quaternary ammonium group of levelers. Electrochemical analyses were performed in three electrodes; Cu rotation disk electrode (Cu RDE, 0.07 cm^2 geometric area) as a working electrode, a wire of Cu as a counter electrode, and Ag/AgCl (KCl-saturated) as a reference electrode. To ensure reproducibility of analysis, Cu RDE was polished with 2000 grit sand paper prior to every analysis. LSV was conducted by scanning the potential from 150 to -350 mV vs.

Ag/AgCl on a scan rate of 1 mV/s. Chronopotentiometry analysis was carried out with all additives injected at 100 s and the current density was applied by 15 mA/cm^2 for 60 min.

2.2. Via-filling test by Cu electrodeposition

In via filling experiments, PCB substrate (2.1 cm x 2.2 cm, Samsung Electro-Mechanics) as the cathode and insoluble IrO_2/Ti electrode filtered by a proton exchange membrane as the anode. The current density was applied to 15 mA/cm^2 for 60 min at the temperature of electrolyte fixed at 25 ℃ by thermostat during the experiment. Vias was reverse-circular truncated cone shaped as 120 and 100 μm at the top and bottom of width with a depth of 100 μm. The cross sectional via was observed by a die of PCB substrate installed in an acrylic resin, which was polished by several abrasive disks and polycrystalline diamond suspension. An optical microscope (ICS-360B, SOMETECH) was used for observation.

3. Results and discussion

3.1.1 Synthesis of Lev-A1

Three choline-based levelers with different number of ammonium functional groups were synthesized. The only difference of three syntheses is different starting materials since three syntheses have the same functional groups but differ in numbers. Therefore, the mechanisms and reagents used in each step are identical for three syntheses.

A synthetic scheme of **Lev-A1** starting from 1-butanol is shown in scheme 1. The first step is allylation of 1-butanol, and allyl intermediate **1** was produced. In the second step, epoxide ring was introduced by oxidizing allyl groups using meta-chloroperoxybenzoic acid (*m*CPBA), and corresponding 2-(butoxymethyl)oxirane **2** was produced. In the third step, epoxide ring was opened with *N,N*-dimethylamine, and 1-butoxy-3-(dimethylamino)propan-2-ol **3** was produced. Finally, allyl functional group and bromide counter ion were introduced at the terminal amine group. Allyl bromide was used to produce *N*-(3-butoxy-2-hydroxypropyl)-*N,N*-dimethylprop-2-en-1-aminium bromide (**Lev-A1**) in overall yield of 47%.

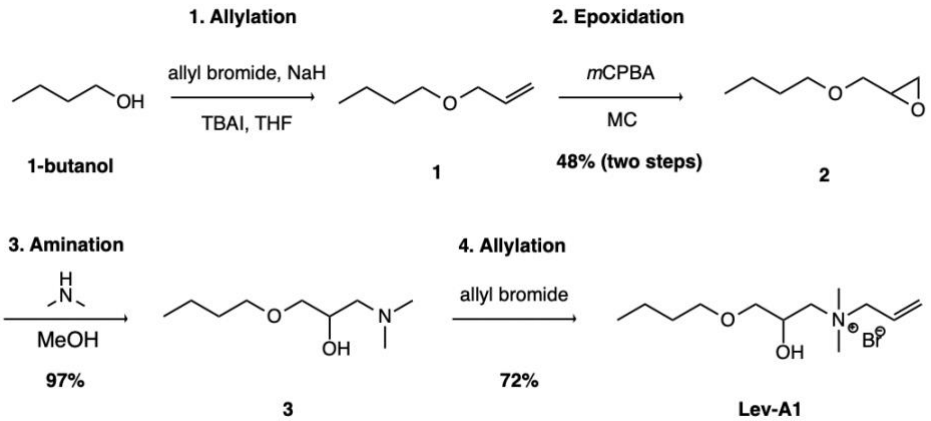

Scheme 1. Synthetic scheme of Lev-A1 from 1-butanol

3.1.2 Synthesis of Lev-A2

A synthetic scheme of **Lev-A2** starting from ethylene glycol is shown in scheme 2. From the starting material ethylene glycol, the same mechanism with **Lev-A1** synthesis consists of allylation, epoxidation, amination, and nucleophilic substitution by allyl bromide was proceeded. The product *N,N'*-((ethane-1,2,diylbis(oxy))bis(2-hydroxypropane-3,1-diyl))bis(*N,N*-dimethylprop-2-en-1-aminium) bromide (**Lev-A2**) was produced with 37% yield.

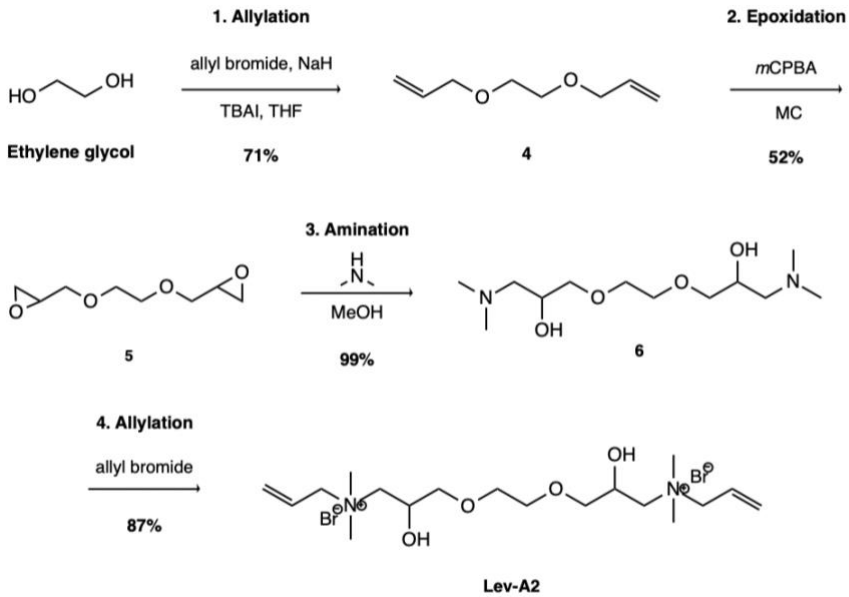

Scheme 2. Synthetic scheme of Lev-A2 from ethylene glycol

3.1.3 Synthesis of Lev-A3

A synthetic scheme of **Lev-A3** starting from glycerol is shown in scheme 3. From the starting material glycerol, the same mechanism with **Lev-A1** synthesis consists of allylation, epoxidation, amination, and nucleophilic substitution by allyl bromide was proceeded. The product *N,N,N''*-((propane-1,2,3-tryltris(oxy)tris(2-hydroxypropane-3,1-diyl))tris(*N,N*-dimethylprop-2-en-1-aminium) bromide (**Lev-A3**) was formed with 47% yield.

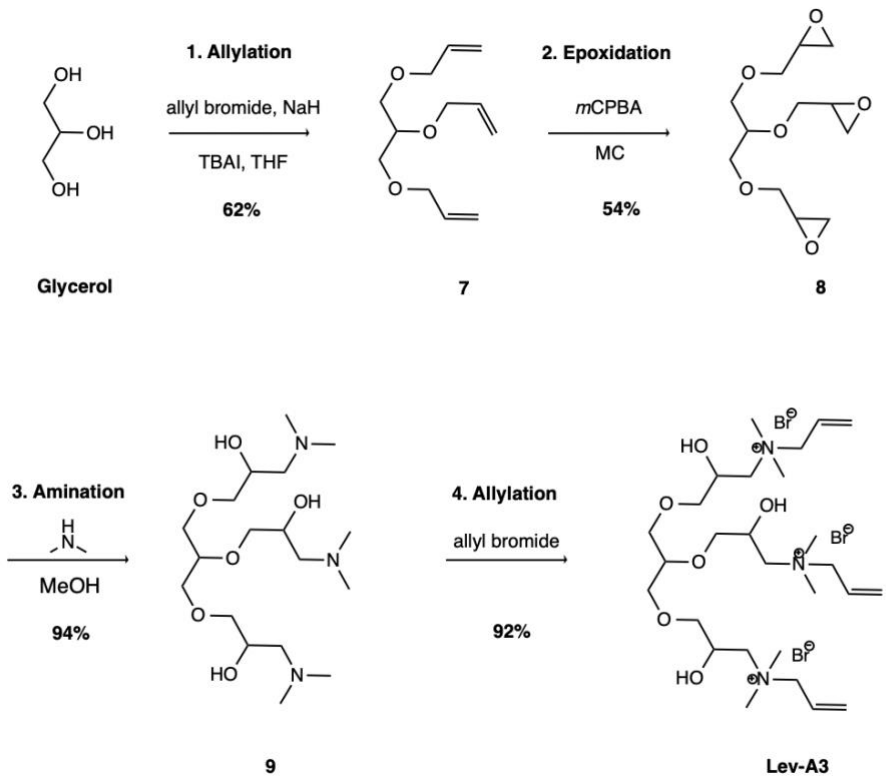

Scheme 3. Synthetic scheme of Lev-A3 from glycerol

3.2. Electrochemical Analyses

From previous research, the influence of quaternary ammonium functional group on the adsorption behavior of leveler was studied.[40,42,44] Several research also identified this influence is related to the convection dependent adsorption.[40-42] Therefore, the inhibition effect of synthesized levelers was compared through LSV by adding levelers only at 100 rpm and 1000 rpm (Fig. 9 and 10). Two rotating speeds of 100 and 1000 rpm were applied to Cu RDE to replicate the convection environments at the bottom and the top of via, respectively. Considering the structure of via, top of via is under the stronger influence of convection than the bottom of via.

LSV and chronopotentiometry were used to analyze the electrochemical behaviors of additives and filling mechanisms. When suppressor and leveler adsorb at the bottom of vias and inhibit Cu reduction, electrons are accumulated on Cu surface, resulting in polarization. Conversely, when adsorption of suppressor and leveler was reduced, their Cu inhibition effect was also decreased, causing depolarization, a positive shift of potential.

Figure. 9 showed that all three levelers exhibited convection dependent adsorption behavior in leveler only additive system. **Lev-A1**, **Lev-A2**, and **Lev-A3** had the greater inhibition effect at the stronger rotating speed (1000 rpm). In addition, onset potentials where the significant increase of the current density starts gradually were shifted negatively from **Lev-A1** to **Lev-A3**. As the formations of effective inhibition layer were observed when potential changes negatively, the onset potential are related to the degree of inhibition effect. More negative onset potential implies the greater inhibition

effect is occurring. Therefore, the strength of inhibition effect increases as the number of quaternary ammonium groups increased. Furthermore, by comparing changes of onset potentials from **Lev-A1** to **Lev-A3** at 100 rpm (ΔV = 85.2 mV, changed from 7.2 to −78 mV) and at 1000 rpm (ΔV = 157 mV, changed from −7 to −150 mV), I found the convection dependent adsorption effect would be greater at the top of via.

Inhibition effect was also observed in three additive system (Fig. 10). Even though onset potential values were all increased significantly, addition of SPS and PPG-PEG-PPG reduced the difference between two convection conditions. Thus, suppressor (PPG-PEG-PPG) would be a key contributing factor of inhibition layer regardless of rotating speeds. In addition, the differences of inhibition effect among levelers were also diminished. At 1000 rpm, the onset potential of **Lev-A1** was −150 mV, and **Lev-A2** and **Lev-A3** had slightly increased value of −170 mV (Fig. 10b). Even though the difference is small, **Lev-A2** and **Lev-A3** could adsorb on Cu surface better than **Lev-A1** due to more binding sites, which resulted in enhanced competitive adsorption with suppressor. **Lev-A2** and **Lev-A3** have linear and triangular adsorption points, respectively. Thus, the number of binding sites would be directly related to inhibition strength. However, the difference of onset potential between **Lev-A2** and **Lev-A3** was barely noticeable at 1000 rpm (Fig. 10b). I assumed that only two of three ammonium groups of **Lev-A3** would participate in adsorption due to inhibition of

suppressor.

Chronopotentiometry was performed to further examine the influence of the number of quaternary ammonium groups on filling efficiency (Fig. 11). The concentration of Lev-A3 was fixed at 7 μM, and SPS concentrations was varied from 3 to12 μM at −15 mA/cm^2 current density. Lev-A3 and SPS were injected at 100 s.

When the rotating speed was 100 rpm, the degrees of depolarization followed the same trend regardless of the concentration of additives. The adsorption of SPS caused rapid depolarization in 1200 s which indicated deactivation of inhibition layer. On the other hand, the inhibition layer was preserved longer at 1000 rpm even though the potential reached as with that ultimately under 100 rpm. Even when the concentrations were adjusted to the quaternary ammonium groups, there was no significant difference found between two convection environments. This chronopotentiometry result was corresponded with via filling test with the concentration matching the equal number of ammonium group.

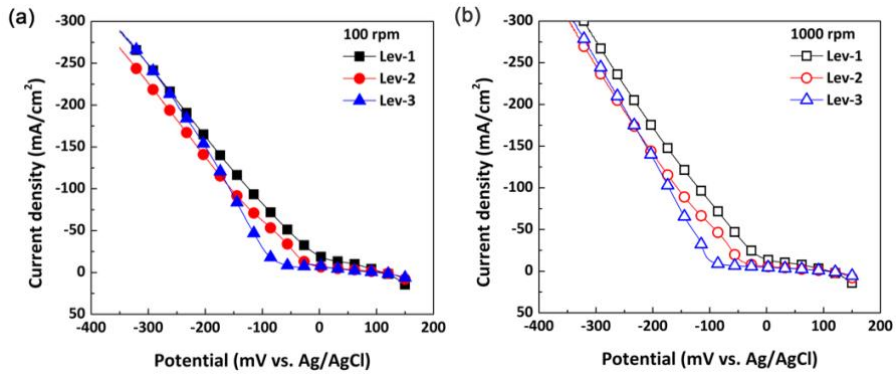

Figure 9. Linear sweep voltammograms of single additive system at two different rotating speeds; (a)100 rpm and (b)1000 rpm. The concentration of levelers was fixed at 7 μM

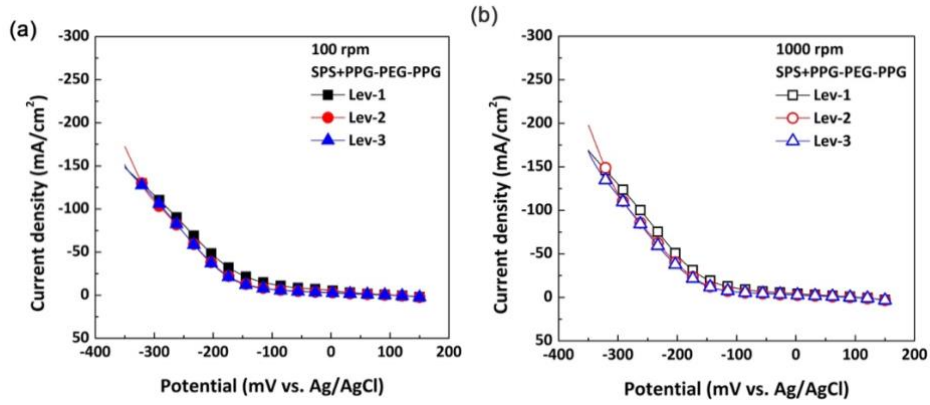

Figure 10. Linear sweep voltammograms of three additive system at two different rotating speeds; (a) 100 rpm and (b) 1000 rpm. The concentrations of levelers, SPS, and PPG-PEG-PPG were fixed at 7 μM, 6 μM, and 100 μM, respectively

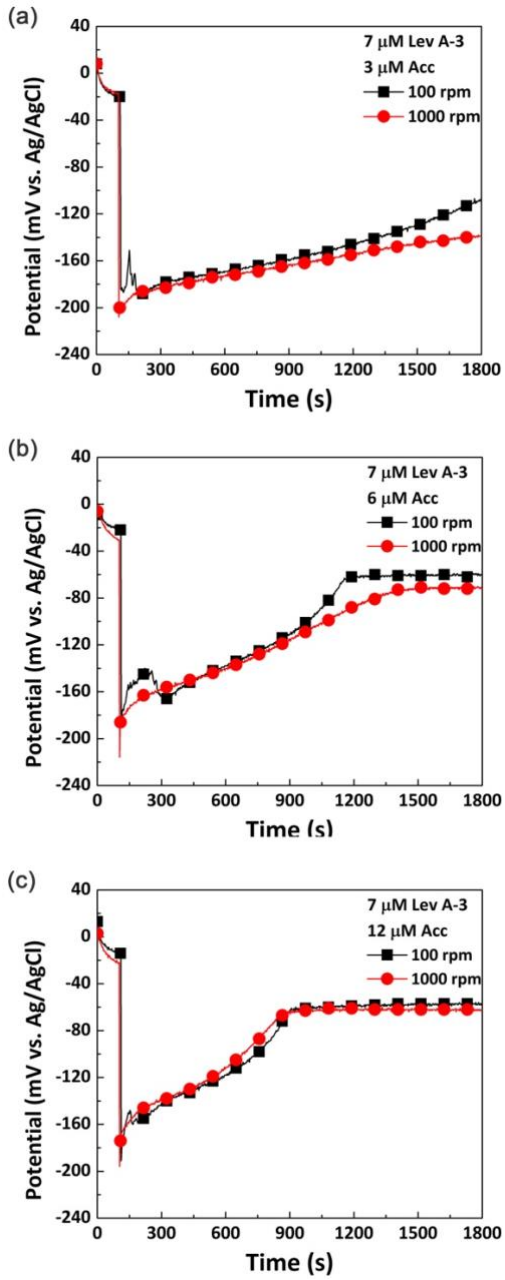

Figure 11. Potential changes with Lev-3 and varying concentration of SPS. The SPS concentrations of (a) 3 μM (b) 6 μM and (c) 12 μM at -15 mA/cm^2 with 7 μM of Lev-A3

3.3. Via-filling test

Via filling test was conducted with the combination of SPS and PPG-PEG-PPG for 60 min deposition time. Filling performance was expressed as thickness ratio (%) when thickness ratio (%) = T_{bottom}/T_{top} x 100.

Among three synthesized levelers, **Lev-A3** exhibited the best filling performance with 217% of the ratio compared to **Lev-A1** (60%) and **Lev-A2** (191%) (Fig. 12). **Lev-A1** resulted in significantly low value which was two-fold as lower than other levelers.

Even though **Lev-A2** and **Lev-A3** showed the similar electrochemical behavior in 3.2, **Lev-A3** resulted in better filling performance with 26% higher ratio. Previously, the inhibition effect of **Lev-A3** was synergistically enhanced with the use of SPS in chronopotentiometry. Therefore, the better filling ratio would be induced because of the interaction between **Lev-A3** and the accelerator.

To examine the effect of the number of quaternary ammonium groups on filling performance in detail, the concentration matching the equal number of ammonium group were adopted. In addition, the same concentration of bromide ion was used in the comparison. Bromide ion since its effect on filling has been known.[48] In previous research, bromide ion could play a role as inorganic leveler since it showed convection enhanced inhibitory effect.[48] On the basis of 7 μM of **Lev-A3**, concentrations of additives were 21 μM of **Lev-A1**,10.5 μM **Lev-A2**, and 21 μM of Br^- were used for via filling test.

However, the filling performance was not improved even when the concentrations of Lev-A1 and Lev-A2 were adjusted to match the number of quaternary ammonium groups (Fig. 13). Unless the adjusted number of quaternary ammonium groups could not result in the same effect, the difference in molecular structure should be considered. Therefore, it would be reasonable to consider the three branches of quaternary ammonium groups in Lev-A3 have significant effects on the inhibition ability. This result also implied that the stability of adsorbed form of Lev-A3 was highly related to the inhibition effect. The inhibition effect was more dependent on three-way branched quaternary ammonium groups than bromide ions.

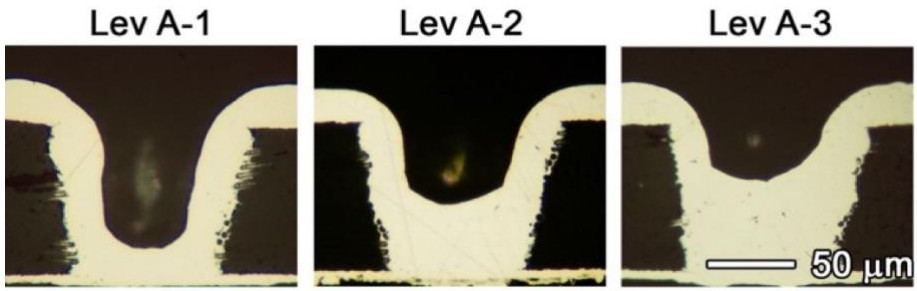

Figure 12. Via filling profiles of three synthesized levelers. Via filling was performed at the current density of −15 mA/cm^2 for 60 minutes. The concentration of levelers was fixed at 7 μM

Table 2. Thickness ratio (%) of three synthesized levelers

Leveler	T_{bottom}	T_{bottom}	Thickness ratio (%)
Lev-A1	29. 8246	17.9825	60
Lev-A2	23.1760	44.2060	190
Lev-A3	28.1938	61.2335	217

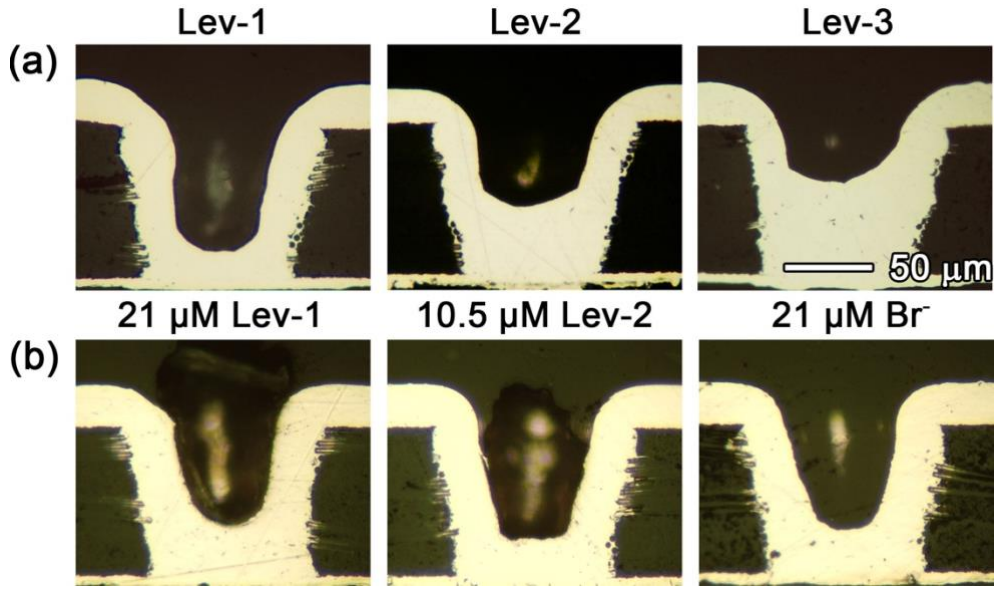

Figure 13. Via filling profiles with the concentrations of equal number of ammonium groups. Via filling was performed at the current density of −15 mA/cm^2 for 60 minutes

4. Conclusion

In this study, three choline-based levelers with different number of quaternary ammonium groups (**Lev-A1, Lev-A2, and Lev-A3**, respectively) were successfully synthesized. The convection dependent adsorption behavior property was observed from all three levelers. Under leveler only additive system, onset potential values were gradually increased as the quaternary ammonium groups increased, and the result implied inhibition effect is enhanced as the number of quaternary ammonium groups are increased. In three additive system (SPS, PPG-PEG-PPG, leveler), strength of inhibition effect depends on the number of quaternary ammonium groups as well. **Lev-A2** and **Lev-A3** showed slightly enhanced inhibition effect than **Lev-A1** which would be related to the competitive adsorption with suppressor. However, the difference between **Lev-A2** and **Lev-A3** was negligible. From the result, I concluded two out of three ammonium groups would participate in adsorption.

Influence of the number of quaternary ammonium groups on inhibition effect was examined by chronopotentiometry and via-filling test. **Lev-A3** showed the best via filling profile compared to the same concentration of **Lev-A1** and **Lev-A2** were applied. However, when the concentration was adjusted to have the same number of quaternary ammonium group, structural stability of **Lev-A3** resulted in better filling profile than other additives. Regardless of matching number of ammonium group, **Lev-A3** exhibited the most effective via filling.

5. Experimental

5.1. General procedure

All the chemicals were obtained from commercial suppliers and were used without further purification. THF was distilled immediately prior to use in the presence of sodium and benzophenone under nitrogen atmosphere. Air moisture-sensitive reactions were conducted under nitrogen atmosphere using oven-dried glassware and standard syringe/septa technique. The reactions were monitored with analytical thin layer chromatography (TLC) using Merck 60, F_{254} glass plates precoated with a 0.25 nm thickness of silica gel. Silica gel 60 F_{254} plates were stained with a p-anisaldehyde or ninhydrin stain solution. Column chromatography was performed on silica gel 60 (70-230 mesh). ^{1}H and ^{13}C NMR spectra were measured at 400 MHz and 100MHz, respectively, in deuterated chloroform ($CDCl_3$) or deuterated methanol (MeOH-d_4) with Brucker Avance-40. The ^{1}H and ^{13}C spectroscopic data were reported in ppm (δ) from the internal standard (TMS, 0.0 ppm) or residual solvent peaks of $CDCl_3$ (7.26 ppm and 77.16 ppm, respectively) or MeOH-d_4 (3.31 ppm and 49.00 ppm, respectively) as follows: chemical shift (integration, multiplicity, and coupling constant in Hz). High resolution mass spectra were measured by fast atom bombardment (FAB) ionization, chemical ionization (CI), or electrospray ionization (ESI) method and analyzed with a magnetic sector mass analyzer or Q-TOF analyzer.

5.2. General synthetic methods

5.2.1 Allylation

1-(allyloxy)butane (1)

To a solution of 1-butanol (1.84 mL, 20 mmol) in dimethylformamide (DMF, 30 mL), sodium hydride (60% NaH, 1200 mg, 30.0 mmol) was slowly added at 0 ℃. The reaction mixture was stirred for 30 min under nitrogen atmosphere. Allyl bromide (2.60 mL, 30 mmol) and tetrabutylammonium iodide (TBAI, $nBu_4N^+I^-$, 792 mg, 2 mmol) were added to the reaction mixture, then the resulting mixture was stirred at room temperature for 6 hrs. The reaction was quenched with distilled water (2 mL), and the resulting mixture was partitioned into diethyl ether (Et_2O, 20 mL) and distilled water (10 mL). The separated organic layer was washed with distilled water (10 mL × 2), and the organic layer was dried over $MgSO_4$, filtered, concentrated under reduced pressure to afford **1** as a crude product.

1,2-bis(allyloxy)ethane (4)

To a solution of ethylene glycol (0.892 mL, 16 mmol) in THF, (20 mL) and DMF (10 mL), 60% NaH (2095 mg, 48 mmol) was slowly added at 0 ℃. The reaction mixture was stirred for 30 min under nitrogen atmosphere. Allyl bromide (4.418 mL, 48 mmol) and TBAI (1269 mg, 48 mmol) were added to the reaction mixture, then the resulting mixture was stirred at room temperature for 6 hrs. The

reaction was quenched with distilled water (2 mL), and the reaction mixture was partitioned into Et_2O (20 mL) and distilled water (10 mL). The separated organic layer was washed with distilled water (10 mL × 2), and the organic layer was dried over $MgSO_4$, filtered, concentrated under reduced pressure to give **4** as a crude product. Though the silica gel chromatography with the gradient elution (Hexane: EtOAc = 16:1 v/v), **4** as a pure product (1.615 g, 71%) as a colorless liquid was obtained; ^{1}H NMR ($CDCl_3$) δ 3.58 (4H, s), 4.00−4.02 (4H, m), 5.14−5.28 (4H, s), 5.85−5.95 (2H, m); ^{13}C NMR (CDCl3) δ 69.6, 72.4, 117.3, 134.9; HRMS ($[M+H]^+$) calcd for $C_8H_{15}O_2^+$ 141.0994, found 141.0992.

3−((1,3−bis(allyloxy)propan−2−yl)oxy)prop−1−ene (7)

To a solution of glycerol (1.46 mL, 20 mmol) in DMF (40 mL), 60% NaH (3600 mg, 4.5 mmol) was slowly added at 0 ℃. The reaction mixture was stirred for 30 min under nitrogen atmosphere. Allyl bromide (7.78 mL, 9 mmol) and TBAI (3568 mg, 9 mmol) were added to the reaction mixture, then the resulting mixture was stirred at the room temperature for 8 hrs. The reaction was quenched with distilled water (5 mL), and the resulting mixture was partitioned into diethyl ether (Et_2O, 20 mL) and distilled water (10 mL). The separated organic layer was washed with distilled water (10 mL × 2), and the organic layer was dried over $MgSO_4$, filtered, concentrated under reduced pressure to give **7** as a crude product. Though the silica gel chromatography with the gradient elution (Hexane : EtOAc = from 16:1 to 4:1 v/v), purified **7** (2.632 g, 62%) as a colorless oil was obtained; ^{1}H NMR ($CDCl_3$) δ 3.50−3.67 (4H, m), 3.68−4.00 (1H, m), 4.01−4.02 (4H, m), 4.02−4.17 (2H, m), 5.14−5.31 (6H, m),

5.86−7.26 (3H, m); ^{13}C NMR ($CDCl_3$) δ 70.3, 71.4, 72.4, 117.0,135.3; HRMS ($[M+H]^+$) calcd for $C_{12}H_{21}O_3^+$ 213.1485, found 213.1492.

5.2.2 Epoxidation

2−(butoxymethyl)oxirane (2)

To the dichloromethane (CH_2Cl_2, 40 mL) solution of the crude product of **1**, *meta*−chloroperoxybenzoic acid (75% *m*CPBA, 4.514 g, 20 mmol) were added and heated under reflux for 6 hrs. The reaction mixture was diluted with CH_2Cl_2 (20 mL), and the resulting solution was washed with an aq. sat. solution of $NaHCO_3$ (20 mL × 3). The organic layer was dried over $MgSO_4$, filtered, and concentrated under the reduced pressure to give **2** as a crude product. Though the silica gel chromatography with the gradient elution (Hexane : EtOAc = from 16:1 to 8:1 v/v), **2** as a pure product (1.255 g, 48% in two steps) as a colorless oil was obtained; ^{1}H NMR ($CDCl_3$) δ 0.91−0.94 (3H, t), 1.37−1.42 (2H, m), 1.54−1.61 (2H, m), 2.60−2.62 (1H, m), 2.80−3.00 (1H, m), 3.13−3.16 (1H, m), 3.37−3.40 (1H, m), 3.44−3.55 (2H, m), 3.61−3.73 (1H, m); ^{13}C NMR ($CDCl_3$) δ 14.0, 19.4, 31.9, 44.5, 51.0, 71.5, 71.6; HRMS ($[M+H]^+$) calcd for $C_7H_{15}O_2^+$ 131.1067, found 131.1066.

1,2−bis(oxiran−2−ylmethoxy)ethane (5)

To the CH_2Cl_2 (40 mL) solution of 1,2−bis(allyloxy)ethane **4**, 75% *m*CPBA 7.842 g, 34.1 mmol) were added and heated under reflux for 6 hrs. The reaction mixture was diluted with CH_2Cl_2 (20

mL) and the resulting solution was washed with an aq. sat. solution of $NaHCO_3$ (20 mL × 3). The organic layer was dried over $MgSO_4$, filtered, and concentrated under reduced pressure to give **5** as a crude product. Though the silica gel chromatography with the gradient elution (Hexane : EtOAc = from 16:1 to 8:1 v/v), **5** as a pure product (1.029 g, 52%) as a colorless oil was obtained; ^{1}H NMR ($CDCl_3$) δ 2.62−2.64 (2H, m), 2.65−2.83 (2H, m), 3.19−3.20 (2H, m), 3.42−3.48 (2H, m), 3.67−3.76 (2H, m), 3.81−3.85 (2H, m); ^{13}C NMR ($CDCl_3$) δ 44.4, 50.9, 70.9, 72.1, 72.2; HRMS ($[M+H]^+$) calcd for $C_8H_{15}O_4^+$ 175.0892, found 176.0012.

2,2',2''−((propane−1,2,3−triyltris(oxy)tris(methylene))tris(oxirane) (8)

To the CH_2Cl_2 (40 mL) solution of 3−((1,3−bis(allyloxy)propan−2−yl)oxy)prop−1−ene **7**, 75% *m*CPBA (12.839g, 55.8 mmol) were added and heated under reflux for 8 hrs. The reaction mixture was diluted with CH_2Cl_2 (30 mL), and the resulting solution was washed with an aq. sat. solution of $NaHCO_3$ (40 mL × 3). The organic layer was dried over $MgSO_4$, filtered, and concentrated under reduced pressure to give **8** as a crude product. Though the silica gel chromatography with the gradient elution (Hexane : EtOAc = from 2:1 to 1:2 v/v), purified **8** (1.743 g, 54%) as a colorless oil was obtained; ^{1}H NMR ($CDCl_3$) δ 0.96−0.99 (3H, t), 1.35−1.42 (2H, t), 2.61−2.63 (3H, m), 2.79−2.82 (3H, dd, J =4.8, 4.4), 3.14−3.18 (3H, m), 3.36−3.54 (2H, m), 3.55−3.67 (5H, m), 3.70−3.73 (1H, m); ^{13}C NMR ($CDCl_3$) δ 43.7, 44.0, 50.4, 50.7, 70.9, 71.0, 71.8, 78.1; HRMS ($[M+H]^+$) calcd for $C_{12}H_{21}O_6^+$ 261.1333, found 261.1338.

5.2.3 Amination

1-butoxy-3-(dimethylamino)propan-2-ol (3)

To the methanol solution of 2-(butoxymethyl)oxirane **2** (1.255 g, 9.64 mmol), *N,N*-dimethylamine (2M in methanol, 14.0 mL, 28 mmol) was added at room temperature, and the reaction mixture was stirred for 12 hrs. After 12 hrs, the reaction mixture was concentrated under reduced pressure. The resulting crude oil was diluted with H_2O (10 mL), and the resulting solution was washed with EtOAc (10 mL × 2). The aqueous layer was concentrated under reduced pressure to yield **3** as a yellowish oil (1.638 g, 97%). The crude product of **3** was sufficiently pure to be used for the next reaction; ^{1}H NMR (MeOH-d_4) δ 0.96-0.97 (3H, t, J = 7.6), 1.37-1.44 (2H, m), 1.57-1.60 (2H, m), 2.30 (6H, s), 2.35-2.46 (2H, m), 3.34-3.43 (2H, m), 3.47-3.51 (2H, m), 3.85-3.89 (1H, m); ^{13}C NMR (MeOH-d_4) δ 14.2, 20.3, 32.8, 45.9, 63.3, 68.8, 72.3, 74.7; HRMS ($[M+H]^+$) calcd for $C_9H_{22}NO_2^+$ 176.1645, found 176.1650.

2,13-dimethyl-6,9-dioxa-2,13-diazatetradecane-4,11-diol (6)

To the methanol solution of 1,2-bis(oxiran-2-ylmethoxy)ethane **5**, *N,N*-dimethylamine (2M in methanol, 10.0 mL, 20 mmol) was added at room temperature, and the reaction mixture was stirred for 12 hrs. After 12 hrs, the reaction mixture was concentrated under reduced pressure. The resulting crude oil was diluted with H_2O (10 mL), and the resulting solution was washed with EtOAc (10 mL × 2). The aqueous layer was concentrated under reduced pressure to yield **6** as a yellowish liquid (1.561 g, 99%). The

crude product of **6** was sufficiently pure to be used for the next reaction; ^{1}H NMR (MeOH−d_4) δ 2.33 (12H, s), 2.45−2.50 (4H, m), 3.31−3.40 (4H, m), 3.42−3.51 (4H, m), 3.64 (4H, s), 3.87−3.93 (2H, m); ^{13}C NMR (MeOH−d_4) δ 46.0, 63.2, 68.9, 71.7, 75.2; HRMS ([M+H]$^{+}$) calcd for $C_{12}H_{29}N_2O_4^{+}$ 265.2049, found 265.2052.

8−(3−dimethylamino)−2−hydroxypropoxy)−2,14−dimethyl−6,10−dioxa−2,14,diazapentadecane−4,12−diol (9)

To the methanol solution 2,2',2''−((propane−1,2,3−triyltris(oxy)tris(methylene))tris(oxirane) **8** (2.490 g, 6.29 mmol), *N,N*−dimethylamine (2M in methanol, 15.0 mL, 30 mmol) was added at room temperature, and the reaction mixture was stirred for 12 hrs. After 12 hrs, the reaction mixture was concentrated under reduced pressure. The resulting crude oil was diluted with H_2O (10 mL), and the resulting solution was washed with EtOAc (10 mL × 2). The aqueous layer was concentrated under reduced pressure to yield **9** as a yellowish oil (4.392 g, 94%). The crude product of **9** was sufficiently pure to be used for the next reaction; ^{1}H NMR (MeOH−d_4) δ 2.30 (18H), 2.36−2.45 (6H, m), 3.43−3.51 (4H, m), 3.54−3.66 (6H, m), 3.68−3.72 (1H, m), 3.92−3.98 (3H, m); ^{13}C NMR (MeOH−d_4) δ 24.2, 45.4, 45.6, 62.7, 68.0, 68.2, 72.3, 74.1, 75.2, 79.8; HRMS ([M+H]$^{+}$) calcd for $C_{18}H_{42}N_3O_6^{+}$ 396.3068, found 396.3078.

5.2.4 Allylation

N-(3-butoxy-2-hydroxypropyl)-*N*,*N*-dimethylprop-2-en-1-aminium bromide (Lev-A1)

To the methanol solution of 1-butoxy-3-(dimethylamino)propan-2-ol **3** (1.638 g, 9.35 mmol), allyl bromide (0.889 mL, 10.3 mmol) was added, and the reaction mixture was stirred for 12 hrs at room temperature. Then, the reaction mixture was concentrated under reduced pressure. The resulting crude oil was diluted with distilled water (10 mL), then the resulting solution was washed with EtOAc (10 mL × 2). The aqueous layer was concentrated under reduced pressure to give **Lev-A1** as a viscous yellowish oil (1.454 g, 72%). The crude product of **Lev-A1** was sufficiently pure enough to be used as an organic additive for the Cu electrodeposition; ^{1}H NMR (MeOH-d_4) δ 0.92-0.96 (3H, t, J = 7.2), 1.35-1.44 (2H, m), 1.53-1.61 (2H, m), 3.17-3.19 (6H, d, J = 8.0), 3.38-3.46 (3H, m), 3.49-3.53 (3H, m), 4.07-4.17 (2H, m), 4.33-4.34 (1H, m), 5.71-5.75 (2H, m), 6.07-6.17 (1H, m); ^{13}C NMR (MeOH-d_4) δ 14.3, 20.3, 32.8, 51.9, 52.2, 66.1, 67.6, 68.8, 72.4, 73.9, 126.6; HRMS ([M-Br]$^+$) calcd for $C_{12}H_{26}BrNO_2^+$ 216.1958, found 216.1964.

N,*N*'-((ethane-1,2-diylbis(oxy))bis(2-hydroxypropane-3,1-diyl))bis(*N*,*N*-dimethylprop-2-en-1-aminium)bromide (Lev-A2)

To the methanol solution of 2,13-dimethyl-6,9-dioxa-2,13-diazatetradecane-4,11-diol **6** (1.561 g, 5.904 mmol), allyl bromide (1.12 mL, 12.99 mmol,) was added, and the reaction mixture

was stirred for 12 hrs at room temperature. Then, the reaction mixture was concentrated under reduced pressure. The resulting crude oil was diluted with distilled water (10 mL), then the resulting solution was washed with EtOAc (10 mL × 2). The aqueous layer was concentrated under reduced pressure to give **Lev-A2** as a viscous yellowish oil (2.601 g, 87%). The crude product of **Lev-A2** was sufficiently pure enough to be used as an organic additive for the Cu electrodeposition; ^{1}H NMR (MeOH-d_4) δ 3.17 (12H, dd, J =7.0), 3.40-3.69 (10H, m), 3.7 (4H, s), 4.11-4.14 (4H, m), 4.37-4.39 (2H, m), 5.72-5.76 (4H, d, J = 6.2), 6.08-6.18 (2H, m); ^{13}C NMR (MeOH-d_4) δ 51.9, 52.2, 66.1, 67.6, 69.0, 71.8, 74.4, 126.6, 129.6; HRMS ([M-Br]$^{+}$) calcd for $C_{18}H_{38}BrN_2O_4^{+}$ 426.2009 found 425.2100.

N,N',N''-((propane-1,2,3-triyltris(oxy))tris(2-hydroxypropane-3,1-diyl))tris(N,N-dimethylprop-2-en-1-aminium)bromide (Lev-A3)

To the methanol solution of 8-(3-dimethylamino)-2-hydroxypropoxy)-2,14-dimethyl-6,10-dioxa-2,14,diazapentadecane-4,12-diol **9** (2.490 g, 6.29 mmol), allyl bromide (1.80 mL, 20.8 mmol) was added, and the reaction mixture was stirred for 12 hrs at room temperature. Then, the reaction mixture was concentrated under reduced pressure. The resulting crude oil was diluted with distilled water (10 mL), then the resulting solution was washed with EtOAc (10 mL × 2). The aqueous layer was concentrated under reduced pressure to give **Lev-A3** as a viscous yellowish oil (4.392g, 92%). The crude product of **Lev-A3** was sufficiently pure enough to be used as an organic additive for the Cu electrodeposition; ^{1}H NMR (MeOH-d_4) δ 3.18-3.21 (18H, d, J =

10.0), 3.41−3.70 (18H, m), 3.71−3.81 (6H, m), 4.12−4.15 (6H, m), 4.39−4.40 (3H, m), 5.73−5.76 (6H, d, J = 11.2), 6.10−6.17 (3H, m); ^{13}C NMR (MeOH−d_4) δ 51.6, 51.9, 65.8, 66.1, 67.3, 68.7, 72.1, 73.4, 7458, 79.5, 126.3, 129.3; HRMS ([M−Br]$^+$) calcd for $C_{27}H_{56}Br_2N_3O_6^+$ 676.2530, found 676.2532.

References

1. Koyanagi, M. *IEICE Electron. Express*, 2015, 12(7), 20152001.

2. Ramm, P., Klumpp, A., Weber, J., Lietaer, N., Taklo, M., De Raedt, W., Fritzsch, T. and Couderc, P. *In 2010 Proceedings of ESSCIRC*, IEEE, 2010, 9-16.

3. Li, Y.; Goyal, D. 3D Microelectronic Packaging: From Fundamentals to Applications; Springer, Switzerland; 2017.

4. Ko, Y.K.; Ko, Y.H; Bang, J.H.; Lee, C.-W. *JWJ*, 2014, 32 (3). 19-26.

5. Kim, H.C.; Kim, M.J.; Kim, J.J. *J. Electrochem. Soc*. 2018, 165(3), D91.

6. Liu, D.; Park, S. *J. of Electron. Packag*. 2014, 136(1).

7. Jun, H.; Cho, J.; Lee, K.; Son, H.Y.; Kim, K.; Jin, H.; Kim, K. *In 2017 IEEE International Memory Workshop*; IEEE, 2007,1-4.

8. Lee, J.C.; Kim, J.; Kim, K.W.; Ku, Y.J.; Kim, D.S.; Jeong, C.; Yun, T.S.; Kim, H.; Cho, H.S.; Oh, S.; Lee, H.S. *In 2016 International SoC Design Conference*; IEEE, 2016, 181-182.

9. Meier, D.J.; Schmidt, S.H. *CIRCUITREE-CAMPBELL-*, 2022, 15, 22-22.

10. Moon, J.H.; Shin, J.; Kim, T.H; Song, D.; Cho, E. *J. Electroanal. Chem.* 2020, 871, 114318.

11. Kamto, A.; Liu, Y.; Schaper, L.; Burkett, S.L. *Thin Solid Films.* 2009, 518(5), m1614-1619.

12. Zhang, Y.; Ding, G.; Wang, H.; Cheng, P. *J. Electrochem. Soc.* 2015, 162(9), D427.

13. Yoon, S. W.; Yang, D. W.; Koo, J. H.; Padmanathan, M.; Carson, F. *2009 IEEE International Conference on 3D System Integration*; IEEE, 2009, 1−5.

14. Cheng, Y.L.; Lee, C.Y.; Huang, Y.L. Noble and Precious Metals−Properties, Nanoscale Effects and Applications. 2018. 220−221.

15. Andricacos, P.C.; Uzoh, C.; Dukovic, J.O.; Horkans, J.; Deligianni, H. *IBM J Res Dev.* 1998, 42(5), 567−574.

16. Gonella, R. *Microelectron. Eng.* 2001, 55(1−4), 245−255.

17. Gupta, T. In Copper Interconnect Technology; Springer, New York; 2009, 267−300.

18. Bhattacharyya, B.; Doloi, B. Modern Machining Technology: Advanced finishing processes. 2020. 675−743.

19. Lee, M.H.; Lee, Y.; Kim, J.A.; Jeon, Y.; Kim, M.J.; Kim, Y.G; Kim, J. *J. Electrochi. Acta*. 2022, 419,140389.

20. Moon, J.; Lee, T.Y.; Ahn, H.J.; Lee, T.I.; Hwang, W.S.; Cho, B.J. *IEEE Trans Electron Devices*. 2018, 66(1), 378−382.

21. Hanim, M.A. 3.15 Electroless Plating as Surface Finishing in Electronic Packaging, 2017, 220−229.

22. Kim, M.J.; Kim, H.C.; Kim, J.J. *J. Electrochem. Soc*. 2016, 163(8), D434.

23. Kim, M.J; Kim, J.J. *Korean Chem. Eng. Res*. 2014, 52(1), 26−39.

24. Reid, J. Jpn. *J. Appl. Phys*. 2001, 40(4S), 2650.

25. Sun, J.J.; Kondo, K., Okamura, T.; Oh, S.; Tomisaka, M.; Yonemura, H., Hoshino; M.; Takahashi, K. *J. Electrochem. Soc*. 2003, 150(6), G355.

26. Jhothiraman, J.K.; Balachandran, R. *ACES*, 2019, 9(2), 239−261.

27. Pasquale, M.A.; Gassa, L.M.; Arvia, A. *J. Electrochi. Acta.* 2008, 53(20), 5891−5904.

28. Moon, J.H.; Shin, J.; Kim, T.H; Song, D.; Cho, E. *J. Electroanal. Chem.* 2020, 871, 114318.

29. Lee, Y. Syntheses and Applications of Nitrogen-Containing Compounds: Levelers with Ammonium Substituents for Cu Electrodeposition and Bioactive L-*threo*-β-Hydroxyaspartates from a Common trans-Oxazolidine Intermediate. *(Doctorate, Seoul National University,* 2022*)*, 5-8.

30. Zhu, Q.S.; Toda, A.; Zhang, Y.; Itoh, T.; Maeda, R. *J. Electrochem. Soc.* 2014, 161(5), D263.

31. Moffat, T.P.; Wheeler, D.; Kim, S.K.; Josell, D. *J. Electrochem. Soc.* 2006, 153(2), C127.

32. Moffat, T.P.; Wheeler, D.; Kim, S.K.; Josell, D. *Electrochi. Acta.* 2007, 53(1),145-154.

33. Luo, J.; Li, Z.; Tan, B.; Cui, C.; Shi, M.; Hao, Z. *J. Electrochem. Soc.* 2019, 166(13), D603.

34. Dow, W.P.; Huang, H.S.; Yen, M.Y.; Huang, H.C. *J. Electrochem. Soc.* 2005, 152(6), C425.

35. Kelly, J.J.; Tian, C.; West, A.C. *J. Electrochem. Soc*. 1999, 146(7), 2540.

36. Lee, M.H.; Lee, Y.; Sung, M.; Cho, S.K.; Kim, Y.G.; Kim, J.J. *J. Electrochem. Soc.* 2020, 167(10), 102505.

37. Kim, H.C.; Kim, M.J.; Seo, Y.; Lee, Y.; Choe, S.; Kim, Y.G.; Cho, S.K.; Kim, J.J. *ECS Electrochem. Lett.* 2015, 4(10), D31.

38. Wang, W; Li, Y.B. *J. Electrochem. Soc*. 2008, 155(4), D263.

39. Healy, J.P.; Pletcher, D.; Goodenough, M. *J. Electroanal. Chem.* 1992, 338(1-2), 155-165.

40. Wang, W.; Hua, H.; Yin, L.; He, Y. *J. Electrochem. Soc*. 2014, 161(12), D651.

41. Zhang, Q.; Yu, X.; Hua, Y.; Xue, W. *J. Appl. Electrochem.* **2015**, 45(1), 79-86.

42. Lu, T.; Wang. F.; He, Y. *J. Electrochem. Soc.* **2016**, 163(13), D663.

43. Li, Z.; Tan, B.; Luo, J.; Qin, J.; Yang, G.; Cui, C.; Pan, L. *Electrochi. Acta.* **2022**, 401, 139445.3.

44. Broekmann, P.; Fluegel, A.; Emnet, C.; Arnold, M., Roeger-Goepfert, C.; Wagner, A.; Hai, N.T.M.; Mayer, D., *Electrochi. Acta.* **2011**, 56(13), 4724-4734.

45. Moffat, T.P.; Wheeler, D.; Edelstein, M.D.; Josell, D. *IBM J Res Dev*, **2005**, 49(1), 19-36.

46. Hai, N.T.; Odermatt, J.; Grimaudo, V.; Kräimer, K.W.; Fluegel, A.; Arnold, M.; Mayer, D.; Broekmann, P. *J. Phys. Chem. C.* **2012**, 116(12), 6913-6924.

47. Huang, Q.; Baker-O'Neal; B.C.; Parks, C.; Hopstaken, M; Fluegel, A.; Emnet, C.; Arnold, M.; Mayer, D. *J. Electrochem. Soc.* **2012**, 159(9), D526.

48. Sung, M.; Yoon, Y.; Hong, J.; Kim, M.J.; Kim, J.J. *J. Electrochem. Soc.* **2019**, 166, D546.

Appendices

List of ^{1}H NMR Spectra of selected compounds

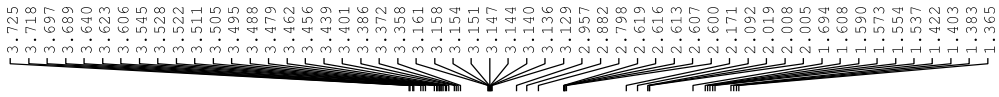
3.725
3.718
3.697
3.689
3.640
3.623
3.606
3.545
3.528
3.522
3.511
3.505
3.495
3.488
3.479
3.462
3.456
3.439
3.401
3.386
3.372
3.358
3.161
3.158
3.154
3.151
3.147
3.144
3.140
3.136
3.129
2.957
2.882
2.798
2.619
2.616
2.613
2.607
2.600
2.171
2.092
2.019
2.008
2.005
1.694
1.608
1.590
1.573
1.554
1.537
1.422
1.403
1.383
1.365

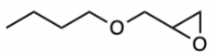

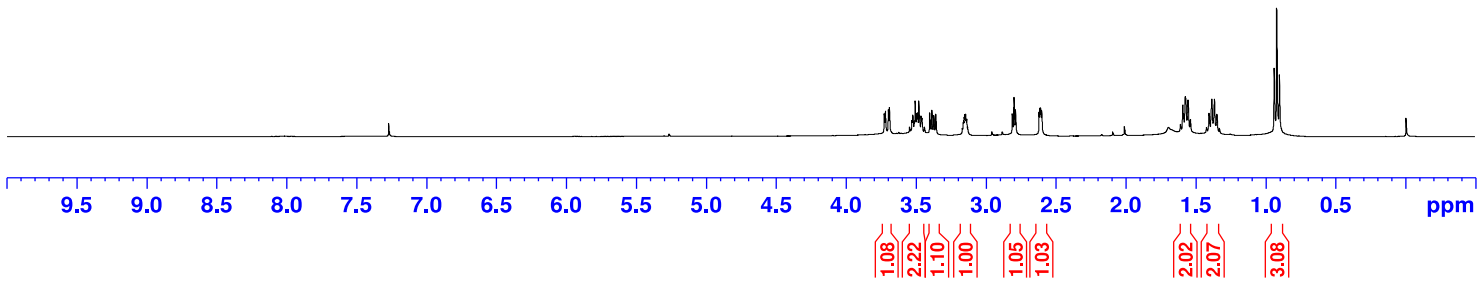
9.5
9.0
8.5
8.0
7.5
7.0
6.5
6.0
5.5
5.0
4.5
4.0
3.5
3.0
2.5
2.0
1.5
1.0
0.5
ppm
1.08
2.22
1.10
1.00
1.05
1.03
2.02
2.07
3.08

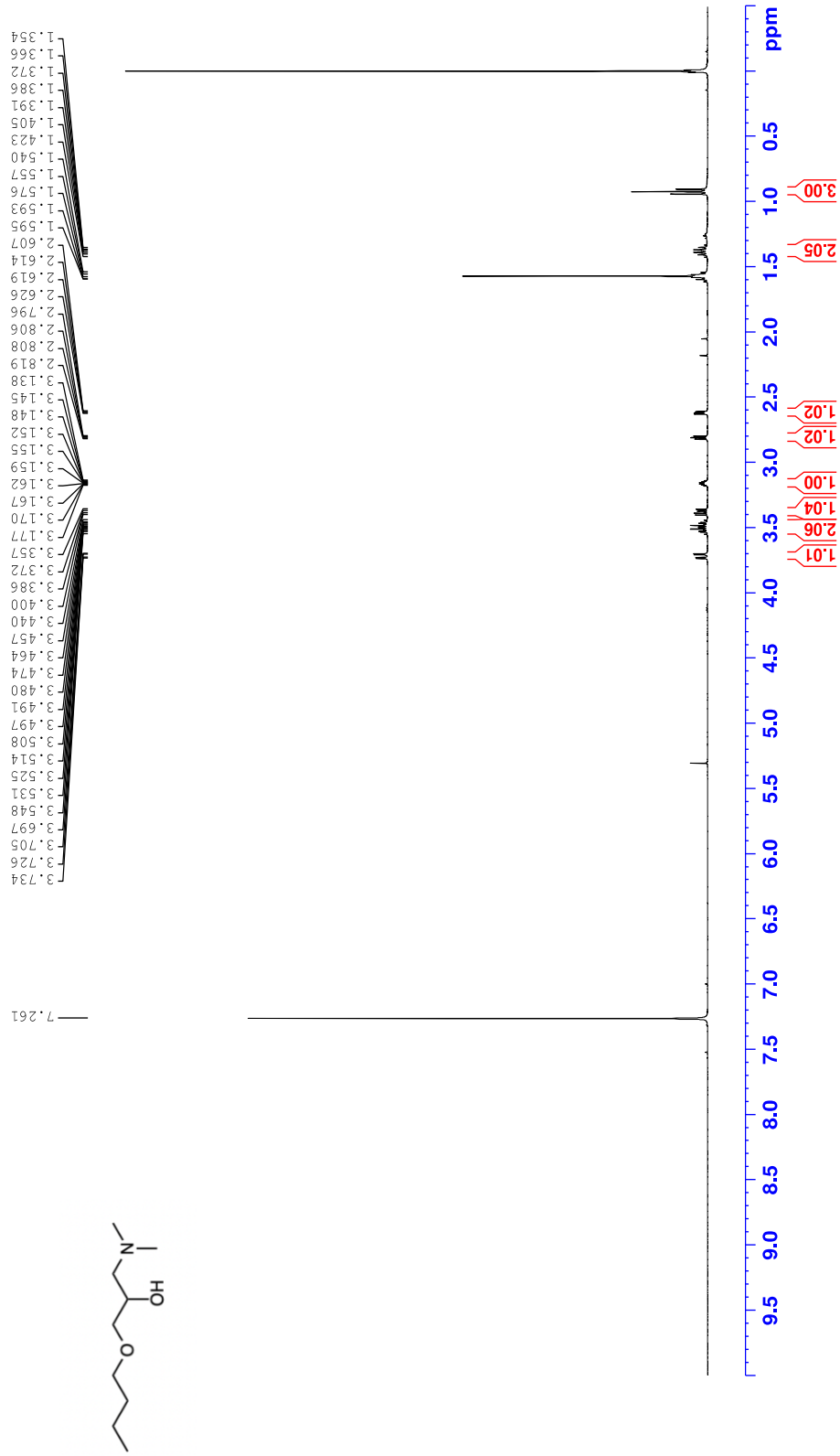
7.261
3.734
3.726
3.705
3.697
3.548
3.531
3.525
3.514
3.508
3.497
3.491
3.480
3.474
3.464
3.457
3.440
3.400
3.386
3.372
3.357
3.177
3.170
3.167
3.162
3.159
3.155
3.152
3.148
3.145
3.138
2.819
2.808
2.806
2.796
2.626
2.619
2.614
2.607
1.595
1.593
1.576
1.557
1.540
1.423
1.405
1.391
1.386
1.372
1.366
1.354
ppm
9.5
9.0
8.5
8.0
7.5
7.0
6.5
6.0
5.5
5.0
4.5
4.0
3.5
3.0
2.5
2.0
1.5
1.0
0.5
1.01
2.06
1.04
1.00
1.02
1.02
2.05
3.00
N
OH
O

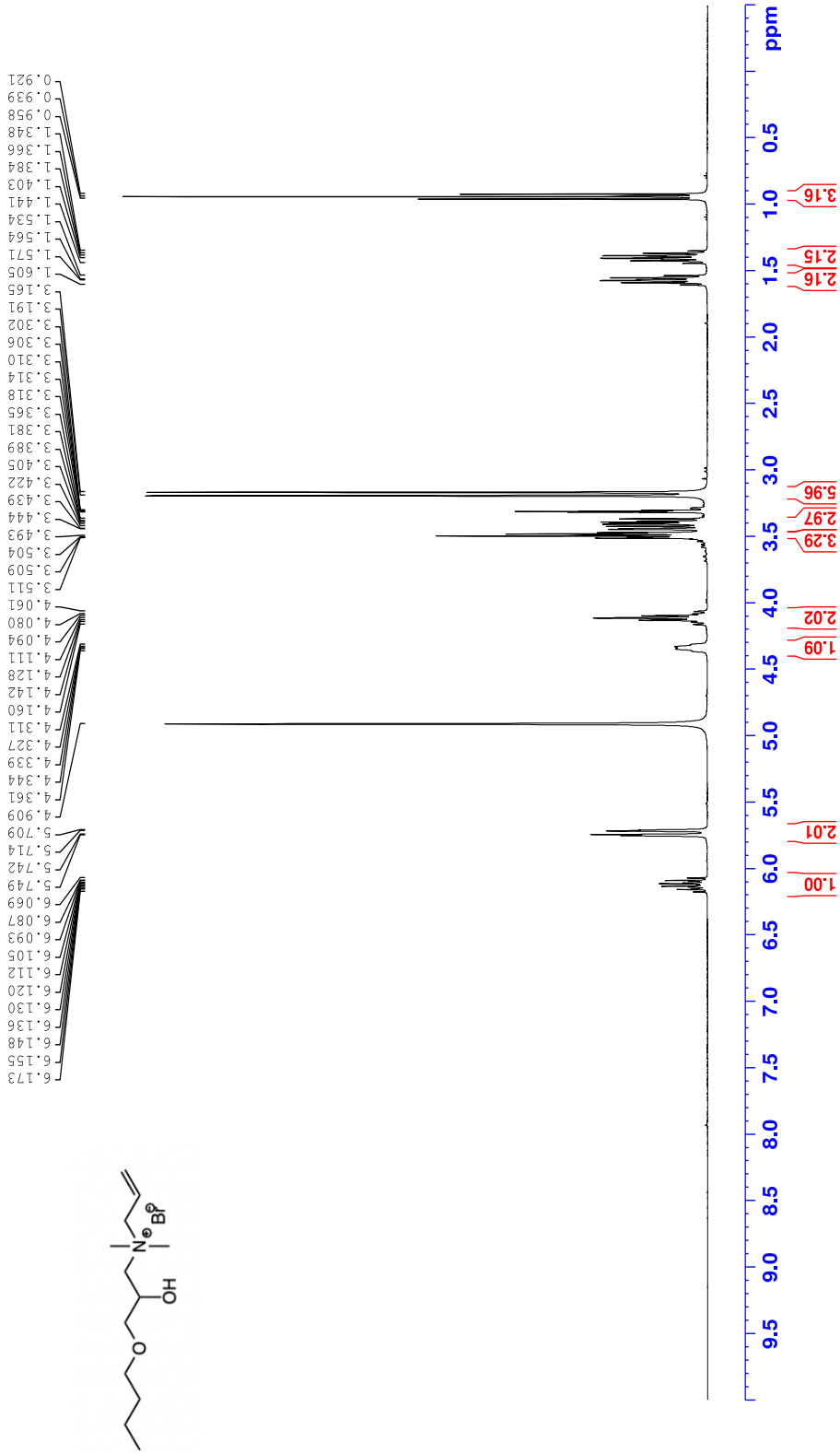
0.921
0.939
0.958
1.348
1.366
1.384
1.403
1.441
1.534
1.564
1.571
1.605
3.165
3.191
3.302
3.306
3.310
3.314
3.318
3.365
3.381
3.389
3.405
3.422
3.439
3.444
3.493
3.504
3.509
3.511
4.061
4.080
4.094
4.111
4.128
4.142
4.160
4.311
4.327
4.339
4.344
4.361
4.909
5.709
5.714
5.742
5.749
6.069
6.087
6.093
6.105
6.112
6.120
6.130
6.136
6.148
6.155
6.173
3.16
2.15
2.16
5.96
2.97
3.29
2.02
1.09
2.01
1.00
ppm
9.5
9.0
8.5
8.0
7.5
7.0
6.5
6.0
5.5
5.0
4.5
4.0
3.5
3.0
2.5
2.0
1.5
1.0
0.5
HO
O
N
BF4

1.563
1.566
1.614
3.532
3.581
3.997
4.000
4.004
4.011
4.014
4.018
5.138
5.141
5.143
5.145
5.148
5.164
5.166
5.169
5.171
5.174
5.223
5.227
5.231
5.235
5.267
5.270
5.274
5.278
5.848
5.862
5.874
5.876
5.888
5.891
5.903
5.905
5.917
5.919
5.931
5.945
7.232
4.03
4.10
4.09
2.00
ppm
9.5
9.0
8.5
8.0
7.5
7.0
6.5
6.0
5.5
5.0
4.5
4.0
3.5
3.0
2.5
2.0
1.5
1.0
0.5

7.284
3.850
3.844
3.837
3.821
3.815
3.808
3.756
3.747
3.745
3.736
3.727
3.722
3.716
3.708
3.702
3.699
3.696
3.686
3.680
3.677
3.668
3.476
3.468
3.461
3.454
3.447
3.439
3.432
3.424
3.203
3.199
3.195
3.187
3.179
2.830
2.820
2.818
2.808
2.645
2.642
2.638
2.635
2.632
2.630
2.625
2.623
2.23
4.46
2.10
2.00
2.12
2.04
ppm
9.5
9.0
8.5
8.0
7.5
7.0
6.5
6.0
5.5
5.0
4.5
4.0
3.5
3.0
2.5
2.0
1.5
1.0
0.5

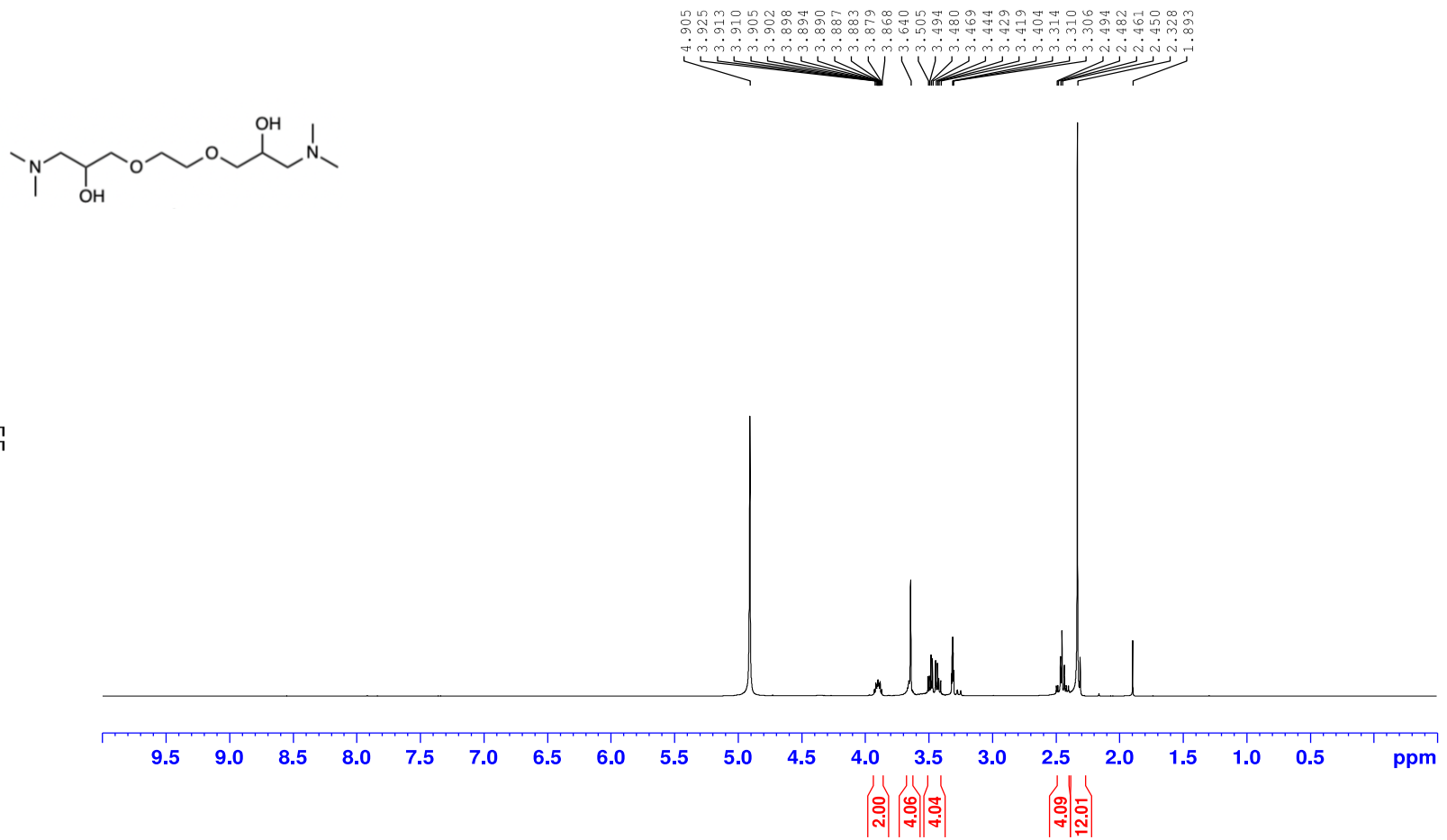
4.905
3.925
3.913
3.910
3.905
3.902
3.898
3.894
3.890
3.887
3.883
3.879
3.868
3.640
3.505
3.494
3.480
3.469
3.444
3.429
3.419
3.404
3.314
3.310
3.306
2.494
2.482
2.461
2.450
2.328
1.893
OH
N
O
O
OH
N
9.5
9.0
8.5
8.0
7.5
7.0
6.5
6.0
5.5
5.0
4.5
4.0
3.5
3.0
2.5
2.0
1.5
1.0
0.5
ppm
2.00
4.06
4.04
4.09
12.01

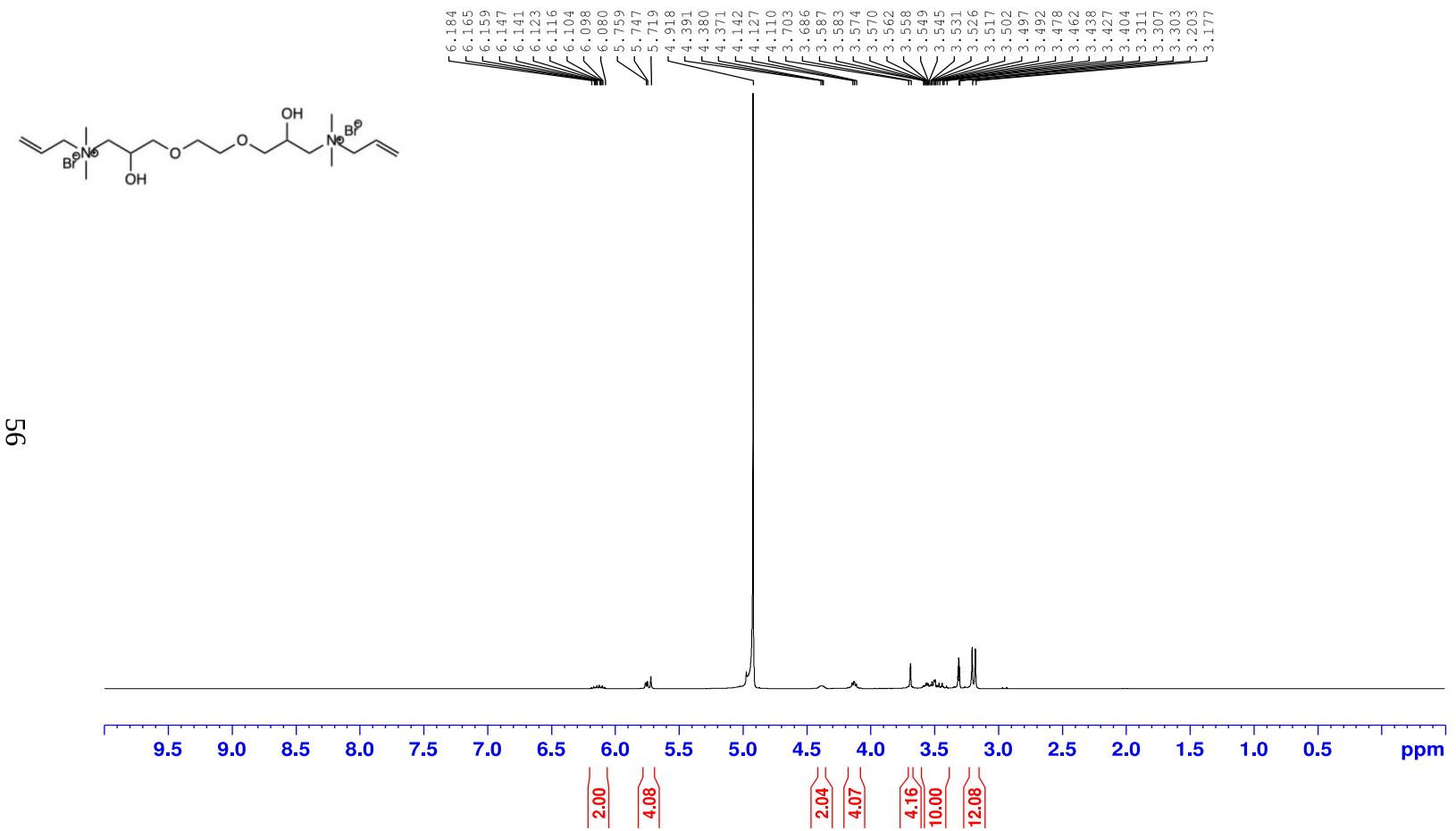
6.184
6.165
6.159
6.147
6.141
6.123
6.116
6.104
6.098
6.080
5.759
5.747
5.719
4.918
4.391
4.380
4.371
4.142
4.127
4.110
3.703
3.686
3.587
3.583
3.574
3.570
3.562
3.558
3.549
3.545
3.531
3.526
3.517
3.502
3.497
3.492
3.478
3.462
3.438
3.427
3.404
3.311
3.307
3.303
3.203
3.177
OH
OH
Br
Br
9.5
9.0
8.5
8.0
7.5
7.0
6.5
6.0
5.5
5.0
4.5
4.0
3.5
3.0
2.5
2.0
1.5
1.0
0.5
ppm
2.00
4.08
2.04
4.07
4.16
10.00
12.08

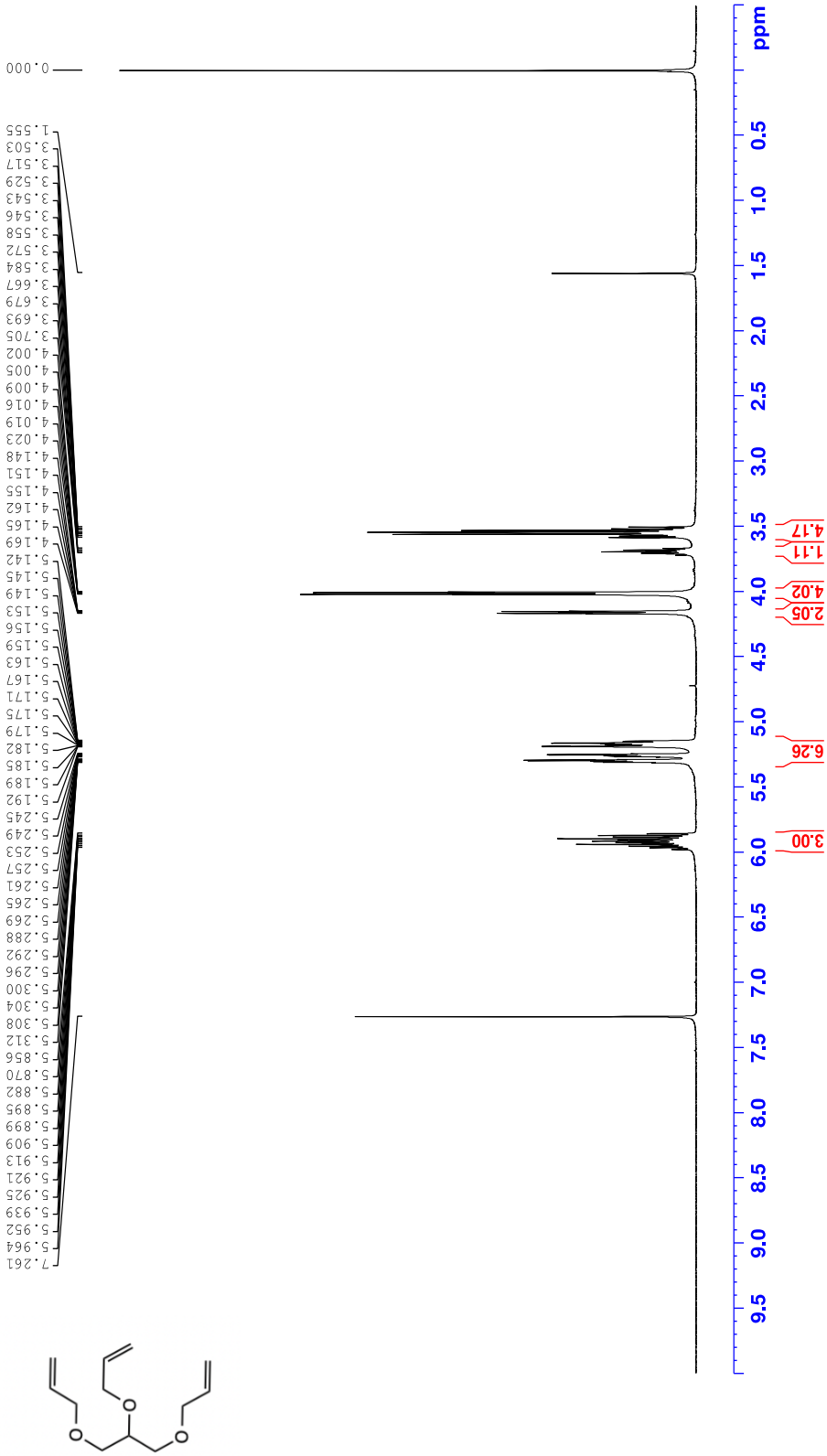
0.000
1.555
3.503
3.517
3.529
3.543
3.546
3.558
3.572
3.584
3.667
3.679
3.693
3.705
4.002
4.005
4.009
4.016
4.019
4.023
4.148
4.151
4.155
4.162
4.165
4.169
5.142
5.145
5.149
5.153
5.156
5.159
5.163
5.167
5.171
5.175
5.179
5.182
5.185
5.189
5.192
5.245
5.249
5.253
5.257
5.261
5.265
5.269
5.288
5.292
5.296
5.300
5.304
5.308
5.312
5.856
5.870
5.882
5.895
5.899
5.909
5.913
5.921
5.925
5.939
5.952
5.964
7.261
ppm
9.5
9.0
8.5
8.0
7.5
7.0
6.5
6.0
5.5
5.0
4.5
4.0
3.5
3.0
2.5
2.0
1.5
1.0
0.5
4.17
1.11
2.05
4.02
6.26
3.00

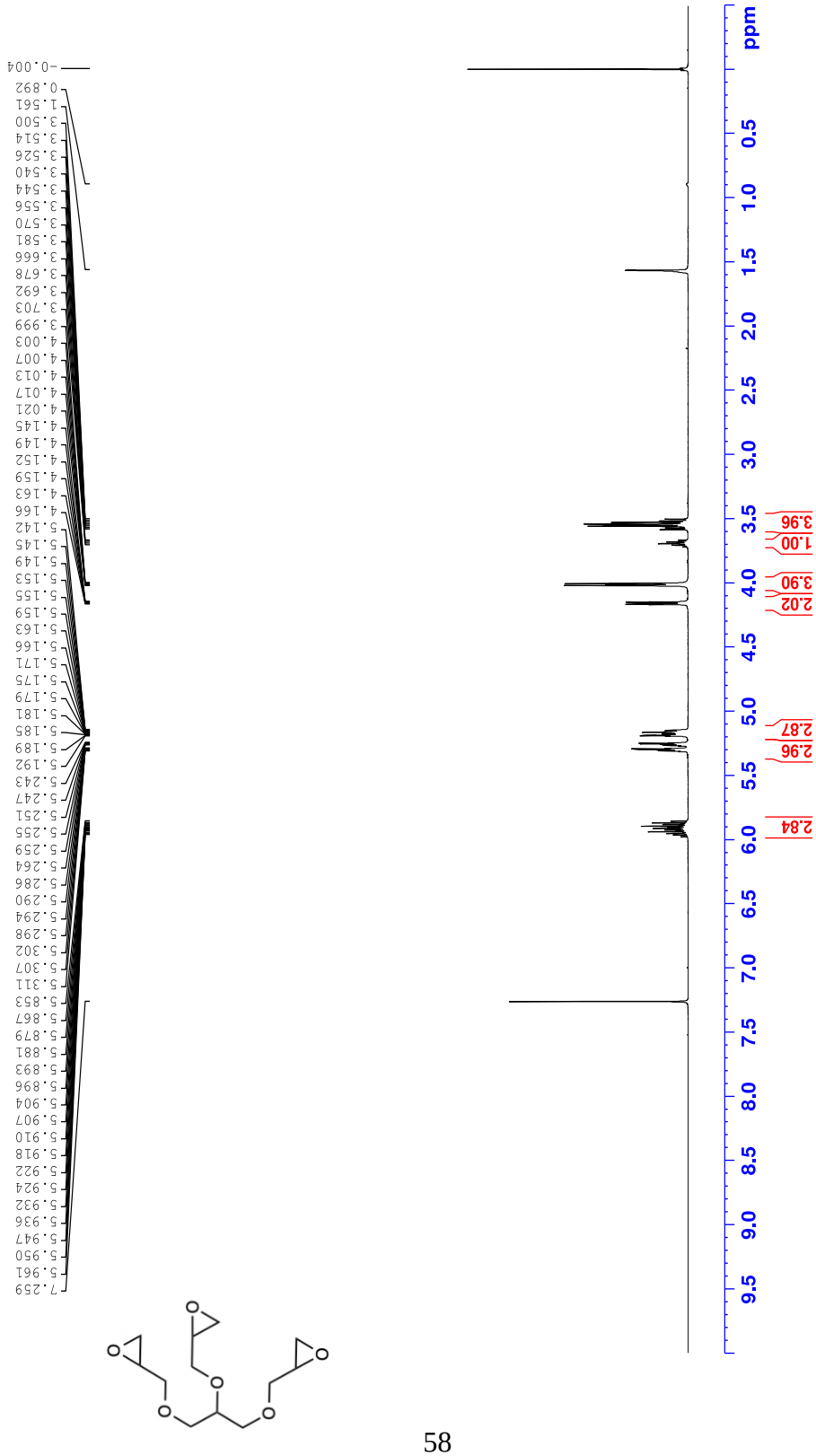
ppm
9.5
9.0
8.5
8.0
7.5
7.0
6.5
6.0
5.5
5.0
4.5
4.0
3.5
3.0
2.5
2.0
1.5
1.0
0.5
3.96
1.00
3.90
2.02
2.87
2.96
2.84

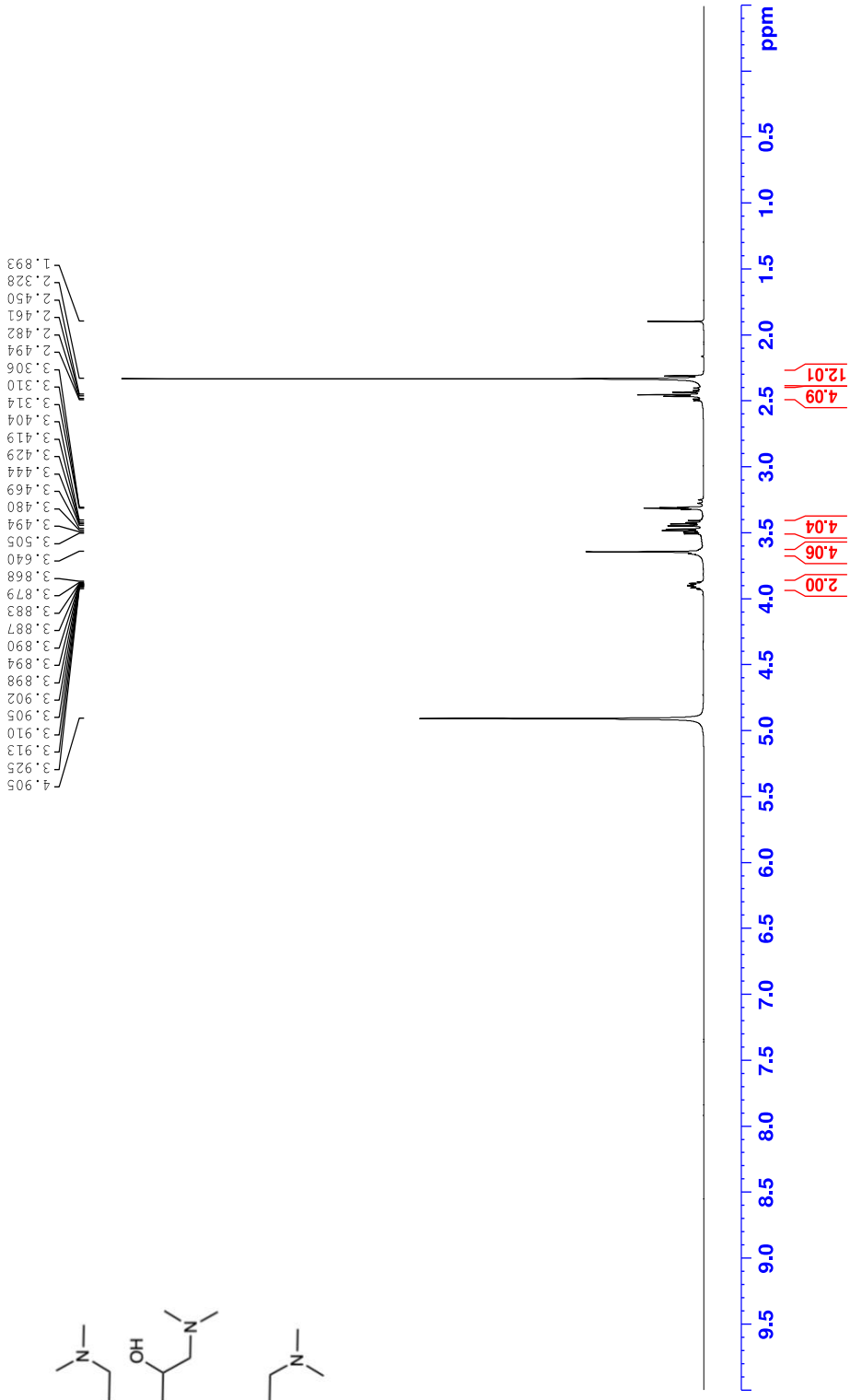
ppm
9.5
9.0
8.5
8.0
7.5
7.0
6.5
6.0
5.5
5.0
4.5
4.0
3.5
3.0
2.5
2.0
1.5
1.0
0.5
2.00
4.06
4.04
4.09
12.01
4.905
3.925
3.913
3.910
3.905
3.902
3.898
3.894
3.890
3.887
3.883
3.879
3.868
3.640
3.505
3.494
3.480
3.469
3.444
3.429
3.419
3.404
3.314
3.310
3.306
2.494
2.482
2.461
2.450
2.328
1.893

N
OH
O
O
O
N
OH
N

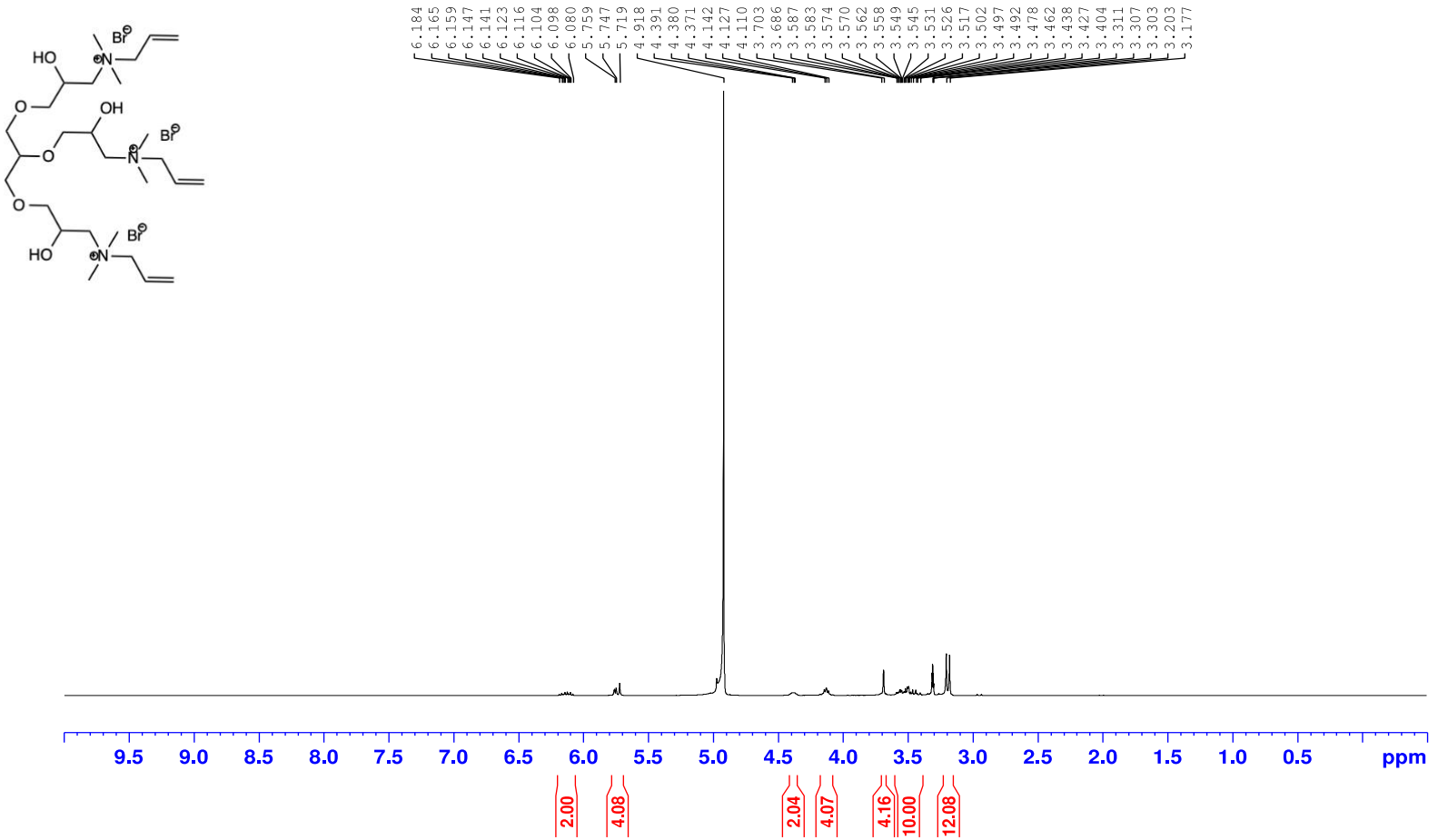
6.184
6.165
6.159
6.147
6.141
6.123
6.116
6.104
6.098
6.080
5.759
5.747
5.719
4.918
4.391
4.380
4.371
4.142
4.127
4.110
3.703
3.686
3.587
3.583
3.574
3.570
3.562
3.558
3.549
3.545
3.531
3.526
3.517
3.502
3.497
3.492
3.478
3.462
3.438
3.427
3.404
3.311
3.307
3.303
3.203
3.177
HO
Br
OH
O
N
9.5
9.0
8.5
8.0
7.5
7.0
6.5
6.0
5.5
5.0
4.5
4.0
3.5
3.0
2.5
2.0
1.5
1.0
0.5
ppm
2.00
4.08
2.04
4.07
4.16
10.00
12.08

List of ^{13}C NMR Spectra of selected compounds

14.008
19.356
31.854
44.454
51.018
71.496
71.557
76.805
77.160
77.440
0 ppm
10
20
30
40
50
60
70
80
90
100
110
120
130
140
150
160
170
180
190

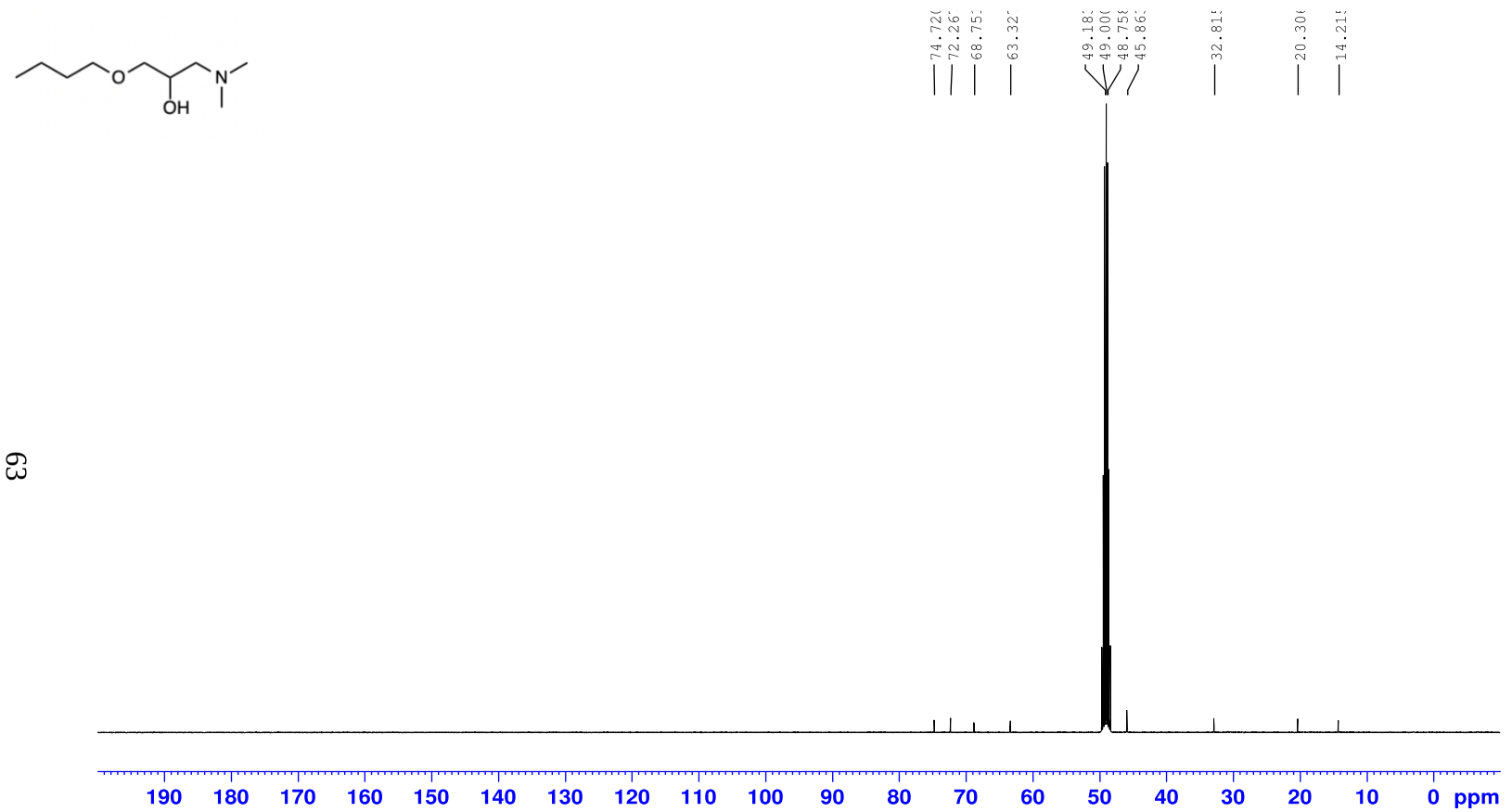
O
N
OH
74.72
72.26
68.75
63.32
49.18
49.00
48.75
45.86
32.81
20.30
14.21
190 180 170 160 150 140 130 120 110 100 90 80 70 60 50 40 30 20 10 0 ppm

63

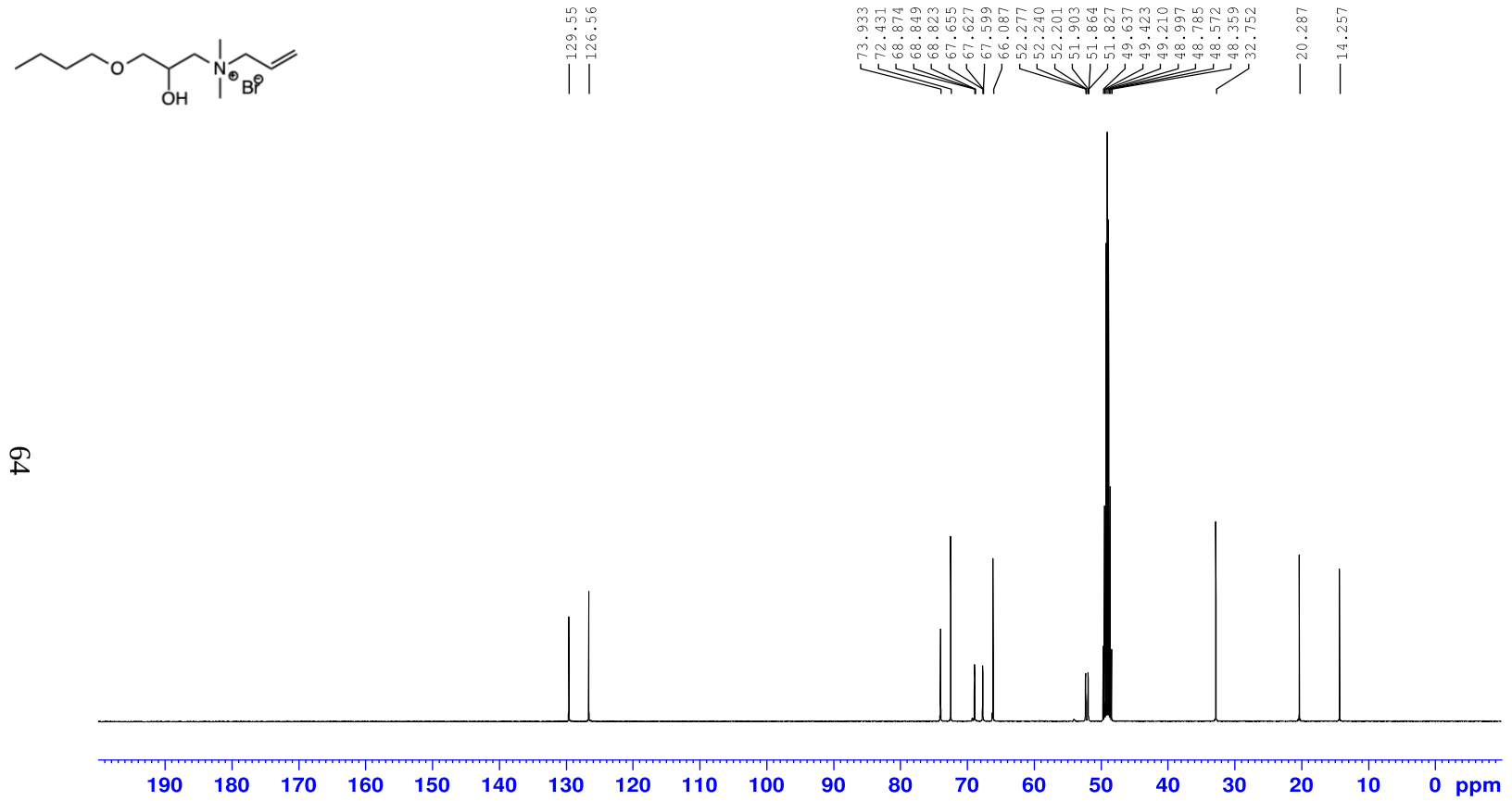
129.55
126.56
73.933
72.431
68.874
68.849
68.823
67.655
67.627
67.599
66.087
52.277
52.240
52.201
51.903
51.864
51.827
49.637
49.423
49.210
48.997
48.785
48.572
48.359
32.752
20.287
14.257
OH
Br
190 180 170 160 150 140 130 120 110 100 90 80 70 60 50 40 30 20 10 0 ppm

64

134.910
117.263
77.472
77.190
76.837
72.439
69.583
190
180
170
160
150
140
130
120
110
100
90
80
70
60
50
40
30
20
10
0 ppm

44.359
50.944
70.854
72.139
72.162
76.834
77.190
77.469
0 ppm
10
20
30
40
50
60
70
80
90
100
110
120
130
140
150
160
170
180
190

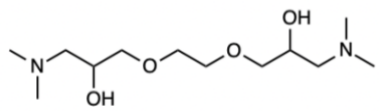
OH
N
O
O
N
OH

75.221
71.700
68.864
63.235
49.613
49.399
49.186
48.762
48.549
48.335
45.977
190
180
170
160
150
140
130
120
110
100
90
80
70
60
50
40
30
20
10
0
ppm

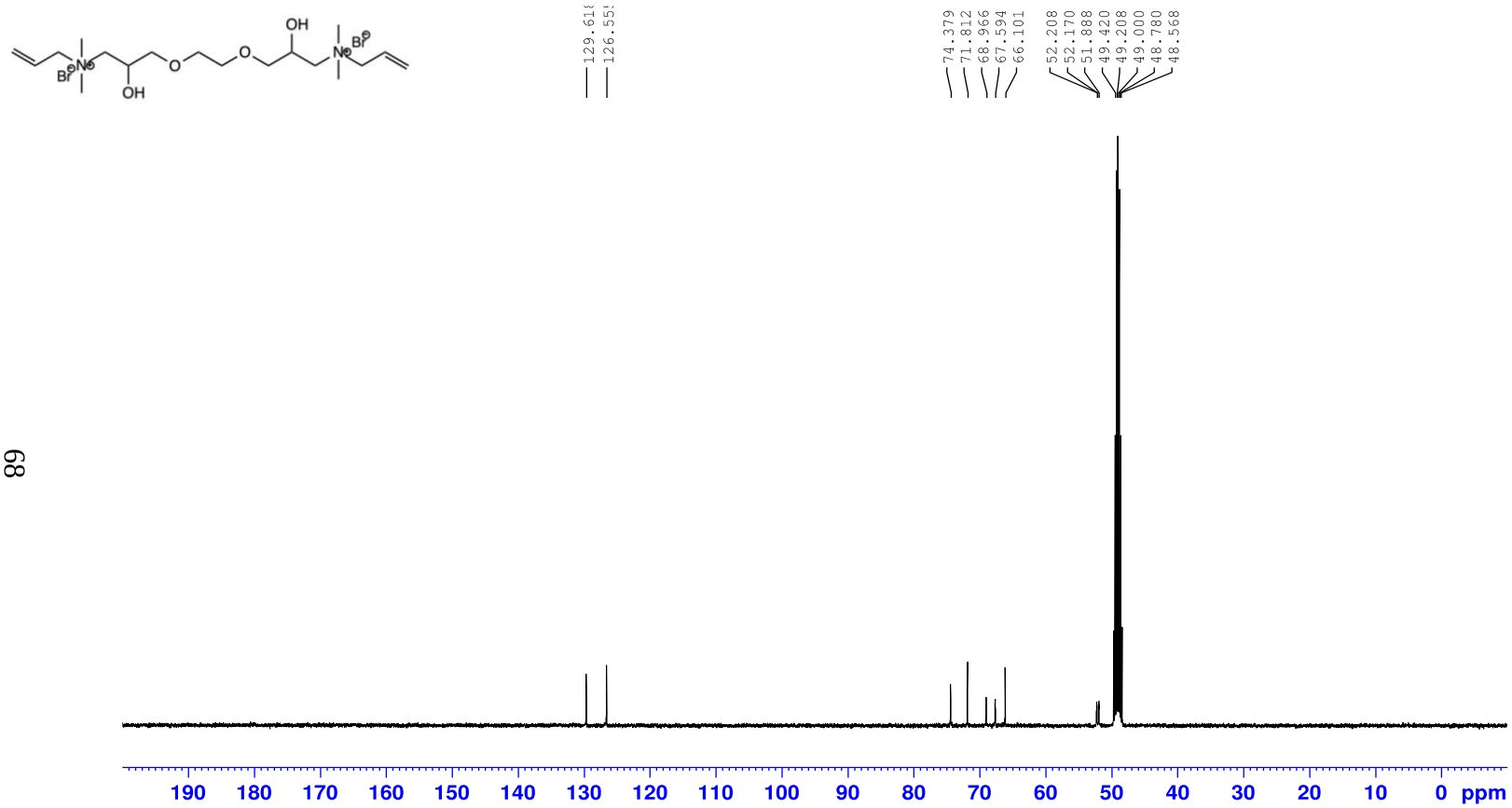
OH
OH
Br
Br
129.61
126.55
74.379
71.812
68.966
67.594
66.101
52.208
52.170
51.888
49.420
49.208
49.000
48.780
48.568
190
180
170
160
150
140
130
120
110
100
90
80
70
60
50
40
30
20
10
0
ppm

69

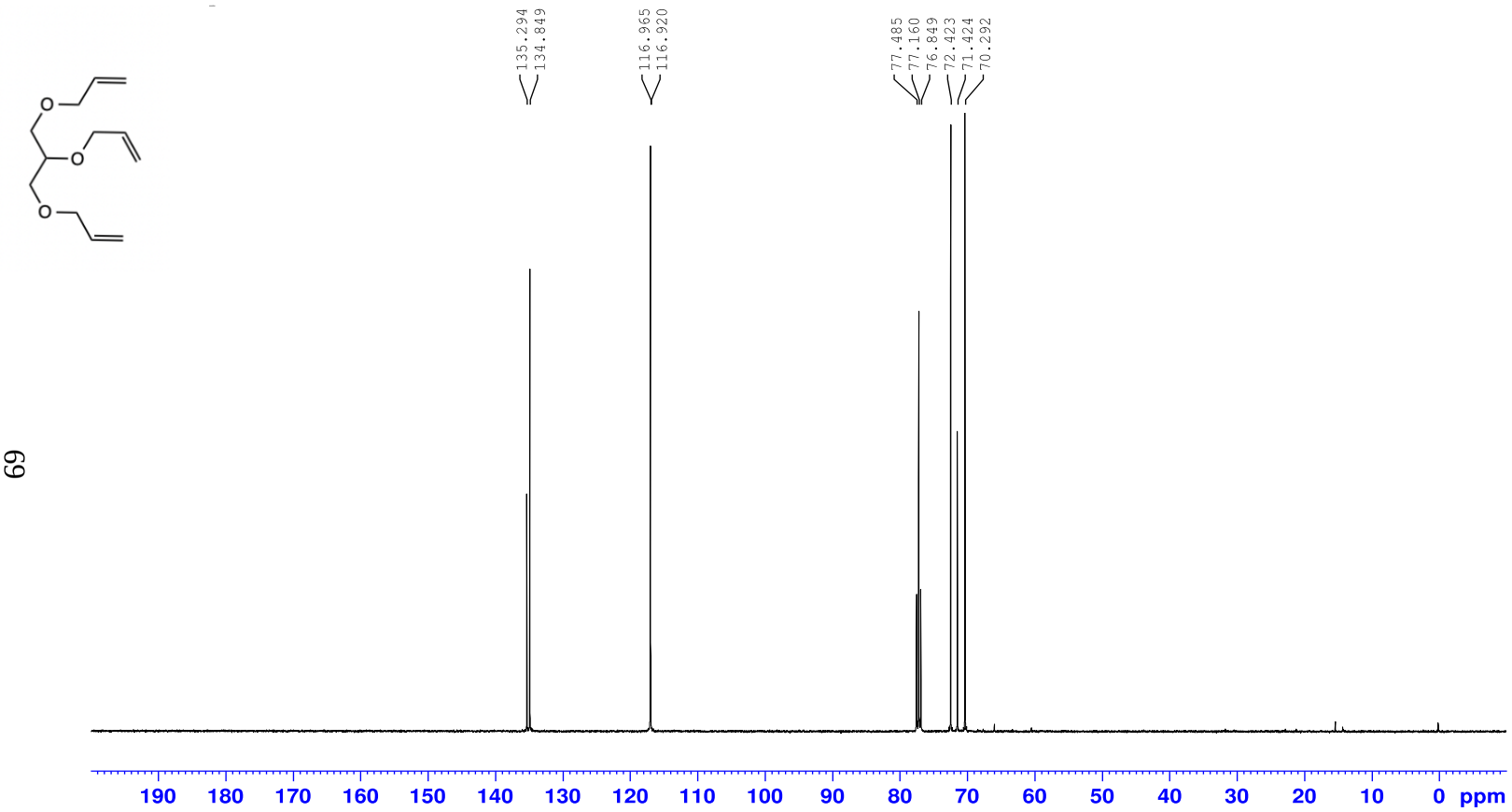
135.294
134.849
116.965
116.920
77.485
77.160
76.849
72.423
71.424
70.292
190 180 170 160 150 140 130 120 110 100 90 80 70 60 50 40 30 20 10 0 ppm

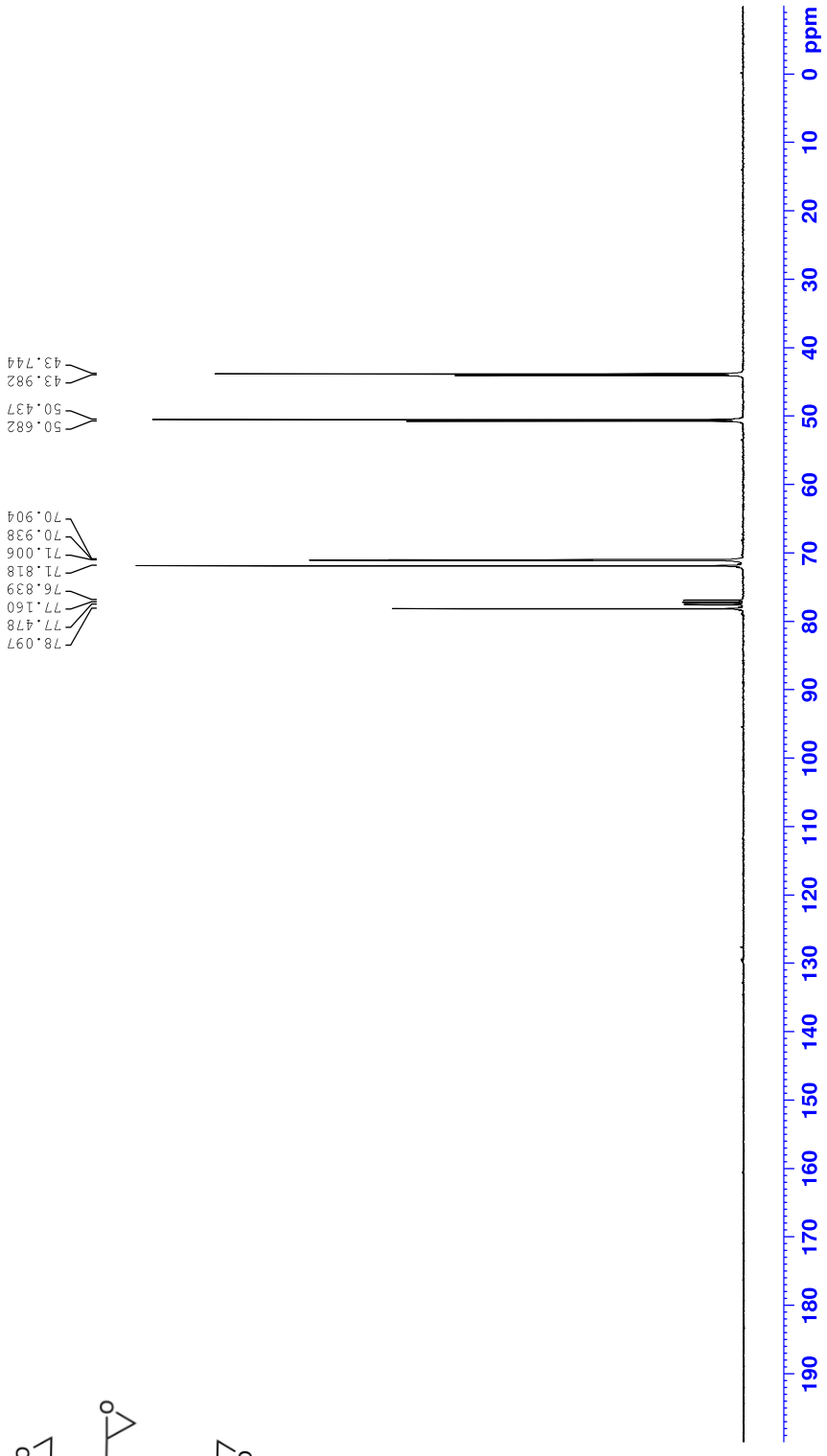
43.744
43.982
50.437
50.682
70.904
70.938
71.006
71.818
76.839
77.160
77.478
78.097
0 ppm
10
20
30
40
50
60
70
80
90
100
110
120
130
140
150
160
170
180
190

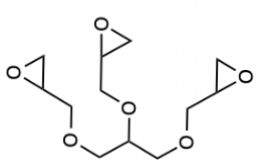

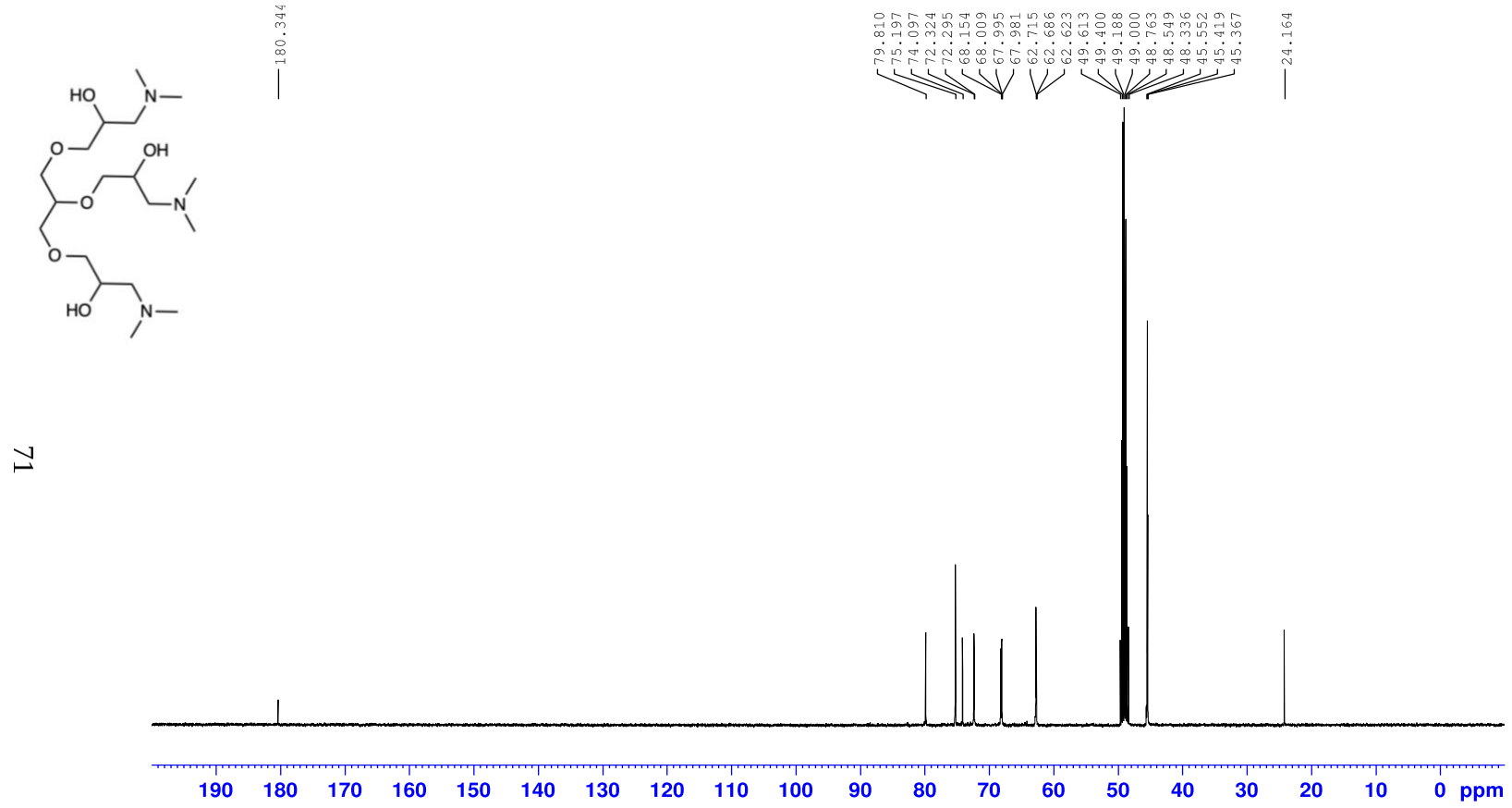
180.344
79.810
75.197
74.097
72.324
72.295
68.154
68.009
67.995
67.981
62.715
62.686
62.623
49.613
49.400
49.188
49.000
48.763
48.549
48.336
45.552
45.419
45.367
24.164
HO
N
O
OH
O
N
O
HO
N
190 180 170 160 150 140 130 120 110 100 90 80 70 60 50 40 30 20 10 0 ppm

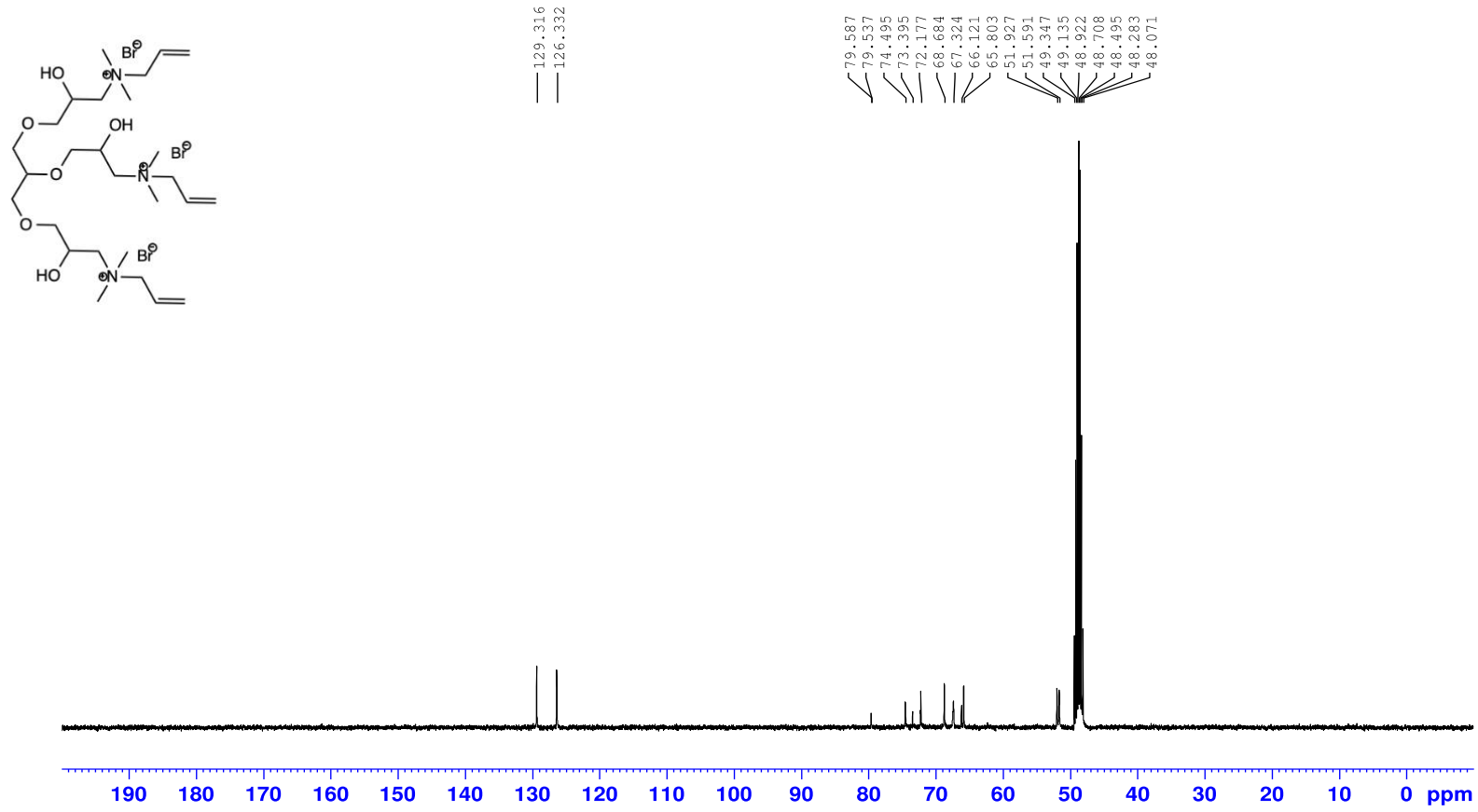
HO
Br
N
O
OH
129.316
126.332
79.587
79.537
74.495
73.395
72.177
68.684
67.324
66.121
65.803
51.927
51.591
49.347
49.135
48.922
48.708
48.495
48.283
48.071
190
180
170
160
150
140
130
120
110
100
90
80
70
60
50
40
30
20
10
0
ppm

국 문 초 록

고성능 반도체를 위한 3D 패키징 기술이 빠르게 발전함에 따라 효율적인 개별 소자들의 전기적 연결 방법 역시 중요해지고 있다. 대표적인 3D 패키징 기술인 실리콘 관통 전극 (TSV)은 적층된 다이들을 관통하는 바이아 홀(via hole)을 도전성 재료를 충전하여 전기적으로 연결하는 기술이다. TSV 기술에서 기기의 신뢰성을 확보하기 위하여 결함 없는 바이아 필링이 무엇보다도 중요하며, 이 과정에서 구리 전해 도금이 주로 사용되고 있다.

결함 없는 구리 전해 도금을 위해서는 도금 첨가제의 사용이 필수적이다. 유기 첨가제 중 하나인 평탄제는 바이아 표면의 위치에 따라 선택적으로 흡착하여 도금의 환원 속도를 조절한다. 이는 평탄제의 대류 의존 흡착 특성에 의해 바이아의 입구에서는 구리 이온의 환원을 억제하고 바이아 바닥에서는 환원을 유도하는 것을 의미한다. 전해 도금에서 평탄제의 영향을 알아보기 위해서는 평탄제의 구조에 따른 활성 분석이 필수적이다. 일반적인 평탄제의 구조는 3 가 아민 또는 4 가 암모늄 치환체를 포함하고 있으며, 이러한 치환체가 평탄제의 대류 의존 흡착 특성에 영향을 준다고 알려져 있다. 따라서 본 학위 논문에서는 서로 다른 개수의 3 종의 4 가 암모늄 치환체를 가지는 평탄제들을 합성하였고 구리 전해 도금에서의 영향을 전기화학적으로 확인하였다.

전기화학분석에서 합성된 모든 평탄제들이 대류 의존 흡착 특성을 나타내었다. 1 개의 암모늄 치환체를 가지는 평탄제 A1 는 각 2 개, 3 개의 암모늄 치환체를 가지는 평탄제 A2 와 평탄제 A3 보다 현저히 낮은 흡착 세기를 보였다. 평탄제 A2 와 평탄제 A3 의 흡착 세기는 큰 차이가 없었지만 마이크로바이아 채움 실험에서는 평탄제 A3 이 근소하게 향상된 결과를 보였다. 암모늄 개수와 평탄제의 구조-

특성의 관계를 알아보기 위해 세 평탄제의 농도를 조절하여 암모늄 그룹의 개수를 동일하게 한 결과, 평탄제 A3 만이 초등각전착을 나타내었다. 이를 통해 암모늄 치환체의 개수 뿐만이 아니라 평탄제 A3 의 구조 또한 구리 이온 흡착에 도움을 준다는 것을 확인하였다. 결과적으로 서로 다른 암모늄 치환체를 가지는 3 종의 평탄제를 성공적으로 합성하였고 구조에 따른 구리도금에서의 특성을 확인하였다.

주요어 : 3D 패키징, 구리 전해 도금, 평탄제, 대류 의존 흡착 특성, 구조 특성 관계, 4 가 암모늄 그룹

학 번 : 2020-26086